AD_____

Award Number: W81XWH-08-1-0537

TITLE: FoxP3 as a missing link between breast cancer and inflammation

PRINCIPAL INVESTIGATOR: Yang Liu, PhD

CONTRACTING ORGANIZATION: The University of Michigan
Ann Arbor, MI 48109

REPORT DATE: September 2009

TYPE OF REPORT: Annual

PREPARED FOR: U.S. Army Medical Research and Materiel Command
Fort Detrick, Maryland 21702-5012

REPORT DOCUMENTATION PAGE

Form Approved
OMB No. 0704-0188

1. REPORT DATE *(DD-MM-YYYY)*	**2. REPORT TYPE**	**3. DATES COVERED** *(From - To)*
01-09-2009	Annual report	1 SEP 2008-31 AUG 2009

4. TITLE AND SUBTITLE
FoxP3 as a missing link between breast cancer and inflammation

5a. CONTRACT NUMBER

5b. GRANT NUMBER
W81XWH-08-1-0537

5c. PROGRAM ELEMENT NUMBER

6. AUTHOR(S)
Yang Liu, PhD (yangl@umich.edu)

5d. PROJECT NUMBER

5e. TASK NUMBER

5f. WORK UNIT NUMBER

7. PERFORMING ORGANIZATION NAME(S) AND ADDRESS(ES)
University of Michigan

Ann Arbor, MI 48109

8. PERFORMING ORGANIZATION REPORT NUMBER

9. SPONSORING / MONITORING AGENCY NAME(S) AND ADDRESS(ES)
U.S. Army Medical Research
and Materiel Command
Fort Detrick,
Maryland 21702-5012

10. SPONSOR/MONITOR'S ACRONYM(S)

11. SPONSOR/MONITOR'S REPORT NUMBER(S)

12. DISTRIBUTION / AVAILABILITY STATEMENT
Approved for public release; Distribution unlimited

13. SUPPLEMENTARY NOTES

14. ABSTRACT
This is the first annual report on the grant "FoxP3 as a missing link between breast cancer and inflammation". Given the importance of both cancer-cell intrinsic (cancer gene) and extrinsic (inflammation) pathways, it is especially intriguing and appropriate to investigate the effect of genetic alteration in genes that have both cancer cell-intrinsic and extrinsic functions, as they may play a unique—and as yet unrecognized-- role in the pathogenesis of breast cancer. The *FoxP3* gene is unique in this regard, in that its alteration can affect both cancer cell-intrinsic function and inflammation. Our proposed work will address the role for inflammation associated with adaptive and innate immune response in the pathogenesis of mammary cancer in female mice with a *FoxP3* mutation. Despite a setback caused by an outbreak of mouse hepatitis virus that lead to termination of the mouse clonies specifically generated for the proposed studies, we made an important observation that targeted mutation of FoxP3 genes in the epithelial cells, resulted in expression of IL-1α and IL1β, key regulators of inflammation. More importantly, expression of IL1b associated with strong inflammation.

15. SUBJECT TERMS
Inflammation, FoxP3, breast cancer risk.

16. SECURITY CLASSIFICATION OF:			**17. LIMITATION OF ABSTRACT**	**18. NUMBER OF PAGES**	**19a. NAME OF RESPONSIBLE PERSON**
a. REPORT	**b. ABSTRACT**	**c. THIS PAGE**			**19b. TELEPHONE NUMBER** *(include area code)*
U	U	U	uu	24	USAMRMC

Standard Form 298 (Rev. 8-98)
Prescribed by ANSI Std. Z39.18

Table of Contents

(4) Introduction

This is the First Report on the grant "FoxP3 as a missing link between breast cancer and inflammation". Apart from the breast cancer cell-intrinsic factors, an important issue is whether inflammation itself is part of the pathogenesis leading to the development and progression of breast cancer. We have hypothesized that FOXP3 mutation will increase inflammatory response in breast cancer. We proposed to test this hypothesis with studies in three specific aims.

Specific aim I. Contribution of innate inflammation to pathogenesis of breast cancer. We have produced $Rag2^{-/-}FoxP3^{sf/sf}$ and $FoxP3^{+/+}Rag2^{-/-}$ mice for cancer incidence. Since the $Rag2^{-/-}$ mice have no adaptive immune system, this model will allow us to determine whether in the absence of adaptive immunity, innate immune system can co-operate with an epithelial cell-intrinsic defect to cause development of mammary tumors in the mice. If so, we will take a genetic and a pharmacological approaches to abrogate the mast cells in order to identify their potential contribution to tumorigenesis.

Specific aim II. What is the significance of Treg-mediated suppression of innate immunity in pathogenesis of mammary tumor? We will adoptively transfer Treg into the $Rag2^{-/-}FoxP3^{sf/sf}$ mice and determine whether it will suppress innate inflammation responsible for the development of breast cancer.

Specific aim III. Define in detail the impact of T-lineage-specific and epithelial cell specific deletion of the FoxP3 gene on the rate of breast cancer in a susceptible background. We will use the mice floxed FoxP3 locus to generate mice with T-lineage-specific or epithelial specific ablation of the FoxP3 gene and monitor the rate and types of breast cancer. The impact of such depletion of T cell activation and functional differentiation at the tumor sites will be determined using intracellular cytokine staining. Should polarized T cells be observed at the tumor sites, the function of the cytokine will be tested by neutralizing antibodies.

Essentially all aims depends on the tumorigenesis of the $Rag2^{-/-Sf/sf}$ mice and observe tumorigenesis in the mice for at least 14 months. Unfortunately, there were a major outbreak of murine hepatitis virus (MHV) infection in the facility. MHV is a mouse pathogen that cause significant alteration in inflammatory response. Because of their immune deficiency, all of the mice generated for the studies are infected, and therefore must be euthanasized in the last year. We are therefore forced to modify research strategy. On one hand, we started regeneration of the mice. At the same time, we have made some very interesting observation on a potential novel mechanism by which FOXP3 regulate inflammatory response. As detailed below.

continues next page

(5) Body of Annual Report

Statement of work

The proposed studies consist of 4 main tasks.

In **task 1**, *we will compare the incidence of tumors in BALB/cRag2$^{-/-}$ FoxP3$^{+/+}$, BALB/cRag2$^{-/-}$ FoxP3$^{sf/sf}$ mice. The mice will be observed for both spontaneous cancer and carcinogen DMBA-induced mammary tumor, using the regiment depicted in Fig. 2. The tumor incidence will be determined first by palpation and confirmed by H&E. Only those samples with confirmed malignancy in mammary tissue will be counted into cancer incidence. We have produced mice of designed genotype and are in the process of expanding the colonies. This will ensure that all the mice can be observed over 24 months.*

This task is essentially finished. We have observed some breast cancer in the *BALB/cRag2$^{-/-}$ FoxP3$^{sf/sf}$* mice. Not tumors were observed in the *BALB/cRag2$^{-/-}$ FoxP3$^{+/+}$* mice. The tumors were identified by H&E studies.

*In **task.2**, we will determine the contribution of mast cells by two approaches. First, we will produce chimera mice using hematopoietic stem cells from new liver of new borne Rag2$^{-/-}$ Kit$^{wt/wt}$ or Kit$^{w\text{-}v/w\text{-}v}$ mutant. The recipient mice Rag2$^{-/-}$FoxP3$^{sf/sf}$ mice and will be irradiated for 500 Rad before receiving 10^6 mononuclear cells from neonate livers. The donor mice will be produced by two steps of breeding. First the Kitwt/w-v mice will be crossed will Rag2$^{-/-}$ mice to generate either Kit$^{wt/w\text{-}v}$Rag2$^{+/-}$ F1 mice. The F1 mice will be crossed to generate F2 neonate mice. PCR based genotyping of neonate liver cells will be used to identifying two types of HSC, Rag2$^{-/-}$Kit$^{wt/wt}$ and Rag2-/-Kit$^{w\text{-}v/w\text{-}v}$. The liver HSC will be injected intravenously, and the chimera mice will be observed for the incidence of cancer.*

This study was not carried out because we have to remove all MHV infected mice in the colony.

*In **task 3,** we will adoptively transfer 10^6 FoxP3-GFP$^+$ cells from BALB/cxB6 FoxP3$^{GFP/wt}$ mice into BALB/c Rag2$^{-/-}$FoxP3$^{sf/sf}$ mice. In order to isolate sufficient number of Treg, we will first purify CD4 T cells by negative selection, and then purify GFP+ cells by FACS sorting. We plan to use 20 recipient mice as recipients, and the other 20 mice will be left untreated. Tumor incidence will be compared.*

This study was not carried out because we have to remove all MHV infected mice in the colony.

*In **task 4,** we will produce lineage-specific knock out of the FoxP3 gene in either T cell-lineage or the epithelial cell lineage. We have backcrossed the FoxP3^{flox} allele into the BALB/c background for six generations, and are in the process of producing the BALB/cFoxP3$^{flox/flox}$ mice. These founders will be crossed with the WSP-Cre transgenic mice to produce FoxP3$^{flox/y}$WASP-Cre$^+$ mice, which will then be crossed with the BALB/cFoxP3$^{flox/flox}$ mice to produce the BALB/c WSP-Cre$^+$FoxP3$^{flox/flox}$ and WSP-Cre$^-$FoxP3$^{flox/flox}$ mice, to be used for tumorigencity studies, as detailed in task I.*
Similar breeding schedules have been planned for the BALB/c LCK-Cre$^+$FoxP3$^{flox/flox}$

This study was not carried out because we have to remove all MHV infected mice in the colony.

Unexpected discoveries

FOXP3 is a transcriptional repressor of IL1α/β expression

The key cytokines for inflammatory response is interleukin 1, which comes in two forms encoded by different genes, *IL1a* and *IL1b*. These genes are normally expressed in macrophages. However, in our analysis of cells with FOXP3 silencing, we observed a major elevation of *IL1A*and *IL1A,* as demonstrated in Fig. 1.

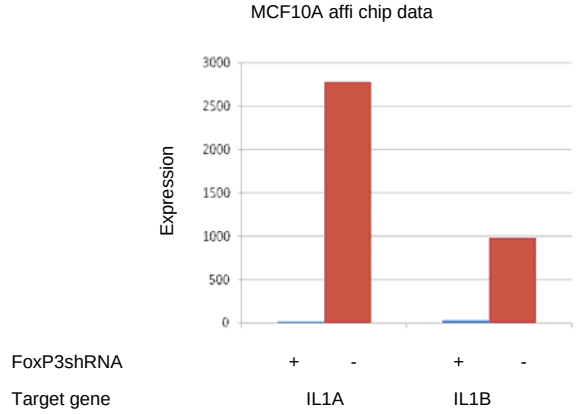

Fig. 1, Gene silencing of FOXP3 by shRNA increases transcripts of IL1A and IL1B. Data shown were relative levels, using control unsilenced cells as 1.0.

Although IL1α protein can induce inflammation without further processing, IL1β is expressed as a precursor, which require further processing, as illustrated in Fig. 2.

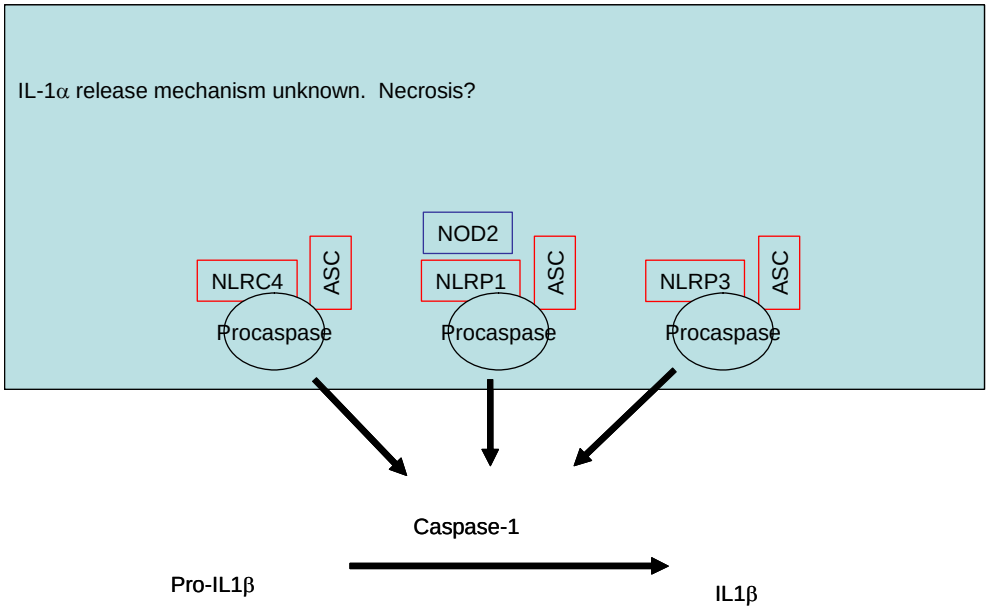

Fig. 2, Diagram of molecules involved in IL1β processing.

We therefore analyzed gene array data to determine if these components are expressed in breast epithelial cells, and if so, whether they are regulated by FOXP3. As shown in Fig. 3, at least two genes are expressed at significant levels. More importantly, they expressions are increased when FOXP3 is silenced.

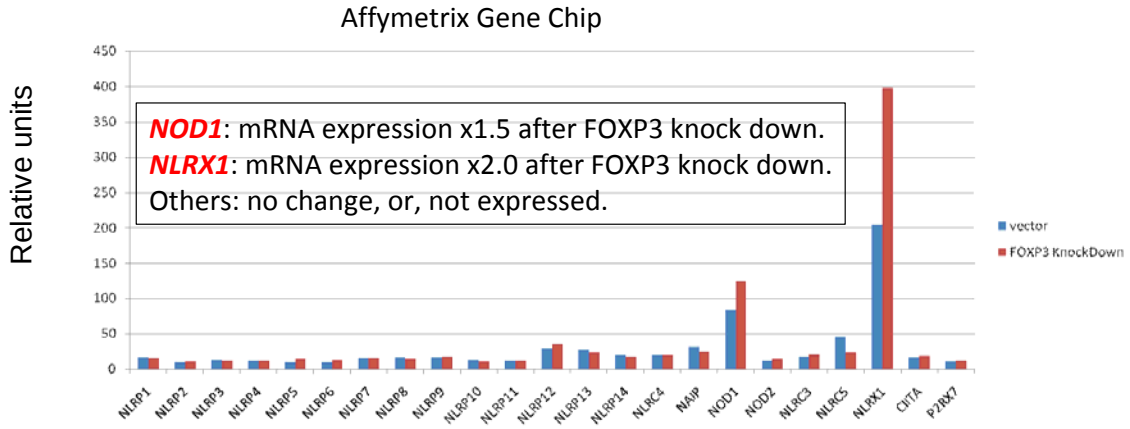

Fig. 3. FoxP3 silencing increase expression of NOD1 (NLRP1) and NLRX1.

To determine whether IL1b is processed and functional in epithelial tissues, we analyzed whether mammary tumors with FOXP3 mutation have mature IL1B protein, and if so, whether their expression correlates with inflammatory response. As shown in Fig. 4, mammary tumor from FoxP3 mutant mice show high levels of mature IL1 in epithelial cells. Correspondingly, large inflammatory infiltrates are found.

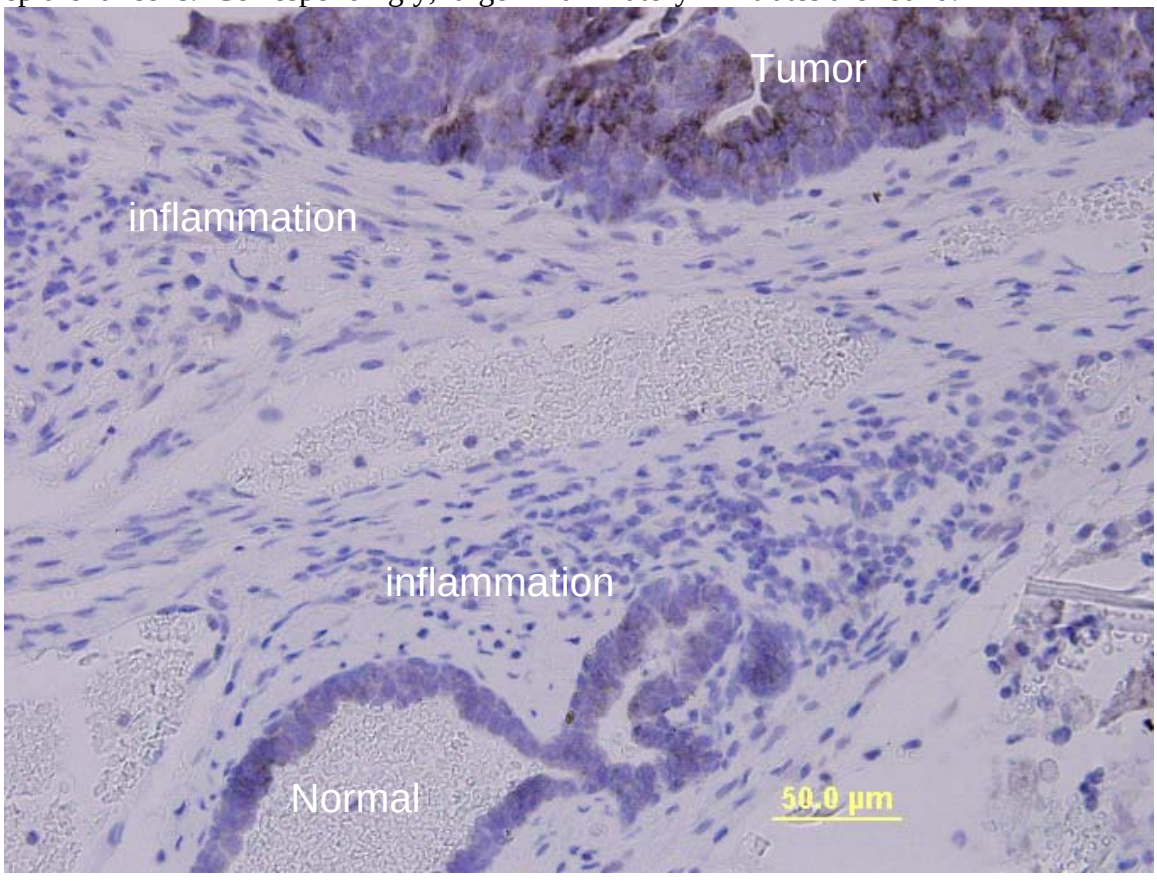

Fig. 4. Expression of mature IL1b in normal and tumor cells of a Foxp3 mutant mice. Presence of IL1b in normal epithelial cells suggest that inflammation can occur prior to tumorigenesis and argue for a role in tumor initiation.

(6) Key Research Accomplishments

Our conclusion that oncogenic mutation directly activates expression of IL1 suggest a novel mechanism of inflammatory response in breast cancer tissue.

(7) Reportable Outcomes:

Manuscripts:

1. Runhua Liu, Lizhong Wang, Guoyun Chen, Hiroto Katoh, Tao Zuo, Chong Chen, **Yang Liu** & Pan Zheng FOXP3 Up-regulates *p21* Expression by Site-specific Inhibition of HDAC 2/4 Association to the Locus. Cancer Res. 2009 Mar 15. 69(6):2252-9. (Appendix 1)
2. Yan Liu, Yin Wang, Weiquan Li, Cindy Wu, Pan Zheng and **Yang Liu**. ATF2 and c-Jun-Mediated Induction of FoxP3 for Experimental Therapy of Mammary Tumor in the Mouse. Cancer Res. 2009 Jul 15;69(14):5954-60. Epub 2009 Jul 7. (Appendix 2).

(8) Conclusions and future plan:

Despite of the set back related to MHV infection, we were able to carry out some work as planned, while making a novel observation which have important implication in mechanism of inflammation in breast cancer. In the next funding period, we hope to complete regeneration of mice and therefore proceed with the proposed work as planned. Furthermore, we hope to pursue the new observation to its completion.

(9) References:

None.

Research Article

FOXP3 Up-regulates *p21* Expression by Site-Specific Inhibition of Histone Deacetylase 2/Histone Deacetylase 4 Association to the Locus

Runhua Liu,[1] Lizhong Wang,[1] Guoyun Chen,[1] Hiroto Katoh,[1] Chong Chen,[1] Yang Liu,[1,2] and Pan Zheng[1,3]

Division of Immunotherapy and [1]Departments of Surgery, [2]Internal Medicine, and [3]Pathology, University of Michigan School of Medicine and Cancer Center, Ann Arbor, Michigan

Abstract

p21 loss has been implicated in conferring oncogenic activity to known tumor suppressor gene *KLF4* and cancer drug tamoxifen. Regulators of *p21*, therefore, play critical roles in tumorigenesis. Here, we report that X-linked tumor suppressor *FOXP3* is essential for *p21* expression in normal epithelia and that lack of FOXP3 is associated with p21 down-regulation in breast cancer samples. A specific *FOXP3* binding site in the intron 1 is essential for *p21* induction by FOXP3. FOXP3 specifically inhibited binding of histone deacetylase 2 (HDAC2) and HDAC4 to the site and increased local histone H3 acetylation. Short hairpin RNA silencing of either HDAC2 or HDAC4 is sufficient to induce *p21* expression. Our data provides a novel mechanism for transcription activation by FOXP3 and a genetic mechanism for lack of p21 in a large proportion of breast cancer. [Cancer Res 2009;69(6):2252–9]

Introduction

As a universal cyclin-dependent kinase inhibitor, p21 plays an important role in preventing cell cycle progression by acting at G_1 checkpoint (1–4). p21 is down-regulated in many types of cancers, including the majority of breast cancer (5–7). Absence of *p21* has been shown to confer oncogenic properties to *KLF4* (8). Moreover, p21 loss is causatively related to the tamoxifen-stimulated growth of breast cancer (9). Surprisingly, *p21* mutation is rarely observed in cancer (10). Instead, *p21* has emerged as a major downstream target of tumor suppressor genes, including *p53* (1, 11, 12), *BRCA1* (13), *CHK2* (14), *KLF4* (15, 16), and *KLF6* (17). Although p53-mediated regulation has been established as a classic example, the lack of correlation between p53 protein levels (usually used as an indication of *p53* mutation) and the down-regulation of p21 would argue strongly that p53 mutation is perhaps not the major underlying cause for p21 loss in breast cancer (5–7). Likewise, although it has been shown that BRCA1-mediated (13) and Chk2-mediated (14) tumor cell cycle arrest and senescence require p21 function, mutations of these two genes had not been established as the genetic cause for the lack of p21 in the tumors. On the other hand, epigenetic factors have been suggested as possible mechanisms of *p21* silencing in breast cancer cells (18–21).

We reported recently that heterozygous *FOXP3* mutation leads to spontaneous development of mammary tumors (22). The significance of *FOXP3* mutation in human is shown by both widespread somatic mutation and deletion of the gene in human breast cancer samples (22). Ectopic expression of the *FoxP3* gene caused profound growth inhibition for breast cancer cell lines both *in vivo* and *in vitro*. Because FoxP3 is a transcription factor, it is important to identify critical targets of FoxP3 that are responsible for the tumor suppressor activity of FoxP3. In this context, we have reported that FoxP3 is a repressor for the *HER-2/ErbB2* and *Skp2* oncogenes (22, 23). Alternatively, it is possible that FoxP3 may activate additional tumor suppressor genes. To test this hypothesis, we used a gene array analysis to identify genes affected by FOXP3. We uncovered several tumor suppressor genes that were induced >2-fold after induction of FOXP3. We focused on *p21*, as it is the most highly induced tumor suppressor and because of its unique role in breast cancer biology. Here, we report that FOXP3 is a potent inducer of *p21* in both normal epithelial cells and malignant breast cancer cell lines. Our data provide a novel mechanism for FOXP3-mediated activation of tumor suppressor gene.

Materials and Methods

Mice. *Rag2*$^{-/-}$*FoxP3*$^{+/+}$ and *Rag2*$^{-/-}$*FoxP3*$^{sf/sf}$ BALB/c mice have been described previously (24). Two-month-old virgin mice were used to analyze the effect of *FoxP3* mutation on *p21* expression and hyperplasia of mammary epithelia. All animal experiments were conducted in accordance with accepted standards of animal care and approved by the Institutional Animal Care and Use Committee of University of Michigan.

Cell culture. Breast cancer cell line MCF-7 and immortalized mammary epithelial cell line MCF-10A were purchased from the American Type Culture Collection. The HO15.19 cell line, which is the c-Myc null derivative of TGR-1 (25, 26), was a kind gift from Dr. John M. Sedivy of Brown University. A previously established tet-off *FOXP3* expression system in the MCF-7 cells was also used (22, 23).

Microarray analysis of FOXP3-regulated genes. The FOXP3 tet-off MCF-7 cells (22, 23) were seeded in six-well plates and cultured with (2.0 μg/mL) and without doxycyclin in the culture media. After 48 h of incubation, cells were washed with ice-cold PBS twice and RNA extraction was performed with RNeasy Mini kit (Qiagen) according to the manufacturer's protocol. Contaminated genomic DNA was eliminated with DNase I (Invitrogen) according to the manufacturer's protocol. We conducted mRNA microarray analyses using HG-U133 Plus 2.0 (Affymetrix) according to the manufacturer's protocol. We used the most current version of ENTREZ gene-based CDFs, as of July 2008, that has been maintained at University of Michigan for accurate analysis (27). dChip software (University of California at Los Angeles Clinical Microarray Core) was used to make a heat map of microarray profiles according to the instruction of the software. Gene expression profiles of FOXP3 tet-off cells cultured with and without

Note: Supplementary data for this article are available at Cancer Research Online (http://cancerres.aacrjournals.org/).

R. Liu and L. Wang, equal contributing authors.

The raw data for microarray analyses have been deposited to MIAExpress (accession no. E-MTAB-73).

Requests for reprints: Pan Zheng, University of Michigan, BSRB 1810, 109 Zina Pitcher Place, Ann Arbor, MI 48109. Phone: 734-615-3158; Fax: 734-763-2162; E-mail: panz@umich.edu.

doi:10.1158/0008-5472.CAN-08-3717

doxycyclin were compared. Differences of mRNA expression levels between FOXP3$^+$ and FOXP3$^-$ cells were calculated by Student's *t* test.

***FOXP3, p21*, and *histone deacetylase* silencing.** Two *FOXP3* short hairpin RNA (shRNA) constructs are *FOXP3*-993 shRNA and *FOXP3*-1355 shRNA (Genbank accession no. NM_014009). Oligonucleotides encoding small interfering RNA (siRNA) directed against *FOXP3* are 5′-GCTTCA-TCTGTGGCATCATCC-3′ for *FOXP3*-993-shRNA [993–1013 nucleotides from transcription starting site (TSS)] and 5′-GAGTCTGCACAAGTGC-TTTGT-3′ for *FOXP3*-1355 shRNA (1355–1375 from TSS). The selected shRNA oligonucleotides were cloned into pSIREN-RetroQ vectors (Clontech) to generate siRNA according to manufacturer's protocol. The human *p21* shRNA (CGCCTCTGGCATTAGAATTATT), human shHDAC2 (shHDAC2-1, CCGACGGTGATATTGGAAATTA; shHDAC2-2, CGGGCAGA-TATTTAAGCCTATT), human shHDAC4 (shHDAC4-1, ACGGCATGACTT-TATATTGTAT; shHDAC4-2, AGACCGGCATGACTTTATATTG), and control lentiviral vectors were purchased from Open Biosystems.

Western blot. The anti-FOXP3 (Abcom, 1:1,000), anti-hFOXY (eBioscience, 1:100), anti-p21 (Cell Signaling, 1:1,000), and anti–β-actin (Sigma, 1:3,000) were used as primary antibodies. Anti-rabbit or mouse IgG horseradish peroxidase–linked secondary antibody at 1:3,000 to 1:5,000 dilutions (Cell Signaling) was used. To ensure equal loading of proteins, the membranes were stripped under the same conditions as described above. They were then incubated with enhanced chemiluminescence reagents (Amersham Biosciences) and exposed to X-ray film for 1 to 5 min.

Chromatin immunoprecipitation. Chromatin immunoprecipitation (ChIP) was carried out according to published procedure (28). Briefly, the FOXP3-transfected tet-off cells were sonicated and fixed with 1% paraformaldehyde. The anti-FOXP3, anti–acetyl-H3 (Cell Signaling), anti–histone deacetylase 1 (HDAC1), anti-HDAC2, anti-HDAC3, anti-HDAC4, anti-HDAC5, anti-HDAC7 (Cell Signaling), and anti-IgG (Santa Cruz Biotechnology) antibodies were used to pull down chromatin associated with FOXP3. The amounts of the specific DNA fragment were quantitated by real-time PCR and normalized against the genomic DNA preparation from the same cells. The ChIP real-time PCR primers are listed in Supplementary Table S3.

Quantitative real-time PCR. Relative quantities of mRNA expression were analyzed using real-time PCR (ABI Prism 7500 Sequence Detection System, Applied Biosystems). The SYBR (Applied Biosystems) green fluorescence dye was used in this study. The primer sequences are listed in Supplementary Table S3.

Immunohistochemistry. Immunohistochemistry was performed by the avidin-biotin complex method. Expression of FOXP3 in human breast cancer or normal tissue samples was determined using immunohistochemistry, as described (22, 23). The p21 mouse monoclonal antibody (Cell Signaling, 1:100) and biotin goat anti-mouse IgG (Santa Cruz, 1:200) were used as secondary antibodies. FOXP3 and p21 staining were scored double blind.

Statistical analysis. Data are shown as means ± SD. Statistical analysis was performed with Student's *t* test for means from two groups. ANOVA test was used for ANOVA between several groups. χ^2 test was used to compare the relationship between the expression of *FOXP3* and *p21*.

Results

***p21* is up-regulated after FOXP3 induction and contributes to its tumor suppressor activity.** We used the MCF-7 cell lines engineered to express FOXP3 in the absence doxycyclin. The cells cultured in the presence or absence of doxyclin for 48 hours were compared with five independent RNA isolates in each group by gene array analysis. A summary of the gene array data, depicting genes that are induced by >2-fold, is shown in Fig. 1*A*. The full data set is shown in Supplementary Tables S1 and S2, and the raw data are deposited to MIAExpress (accession no. E-MTAB-73).

Among the FOXP3-induced genes are several tumor suppressors, including *p18, p21, LAT2,* and *ARHGAPS* (Fig. 1*A*). We have chosen

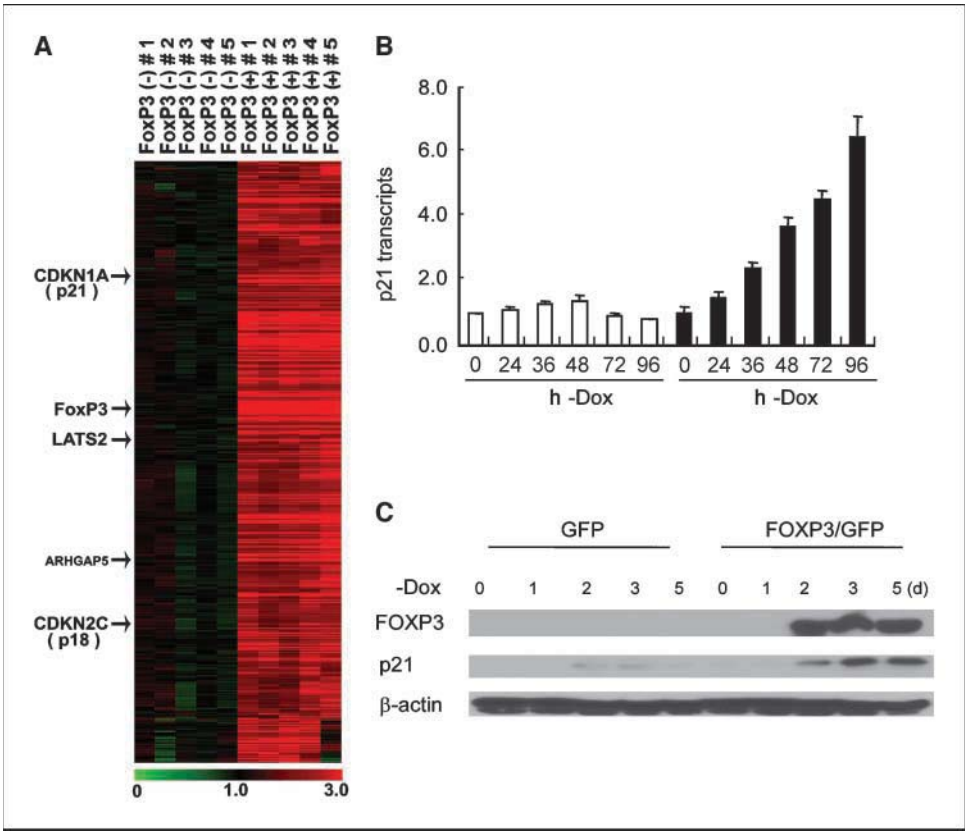

Figure 1. Identification of *p21* as a FOXP3-induced tumor suppressor gene. *A,* gene expression profiles in a panel of five flasks of FOXP3$^+$ cells and five flasks of FOXP3$^-$ cells. Expression values of each row were normalized to the average expression value of each gene among the FoxP3$^-$ cells. Color scales of gene expression levels are indicated at the bottom of the figure. Known tumor suppressor genes are indicated at the left side of the heat map. *B* and *C,* confirmation of *p21* up-regulation by FOXP3. After removing doxycyclin from the medium, the cells were collected at 0, 24, 36, 48, 72, and 96 h and the *FOXP3* expression was measured by real-time PCR (*B*) and Western blotting (*C*). *B,* the mRNA levels of *p21* were measured by real-time PCR for the pBI-GFP vector control cells and pBI-*FOXP3*/GFP cells. The mean of the 0 h is artificially defined as 1.0. *Columns,* mean of three independent experiments; *bars,* SD. *C,* the protein levels of FOXP3 and p21 were detected in the GFP control and FOXP3/GFP cells by Western blotting without doxycyclin from 0 to 5 d.

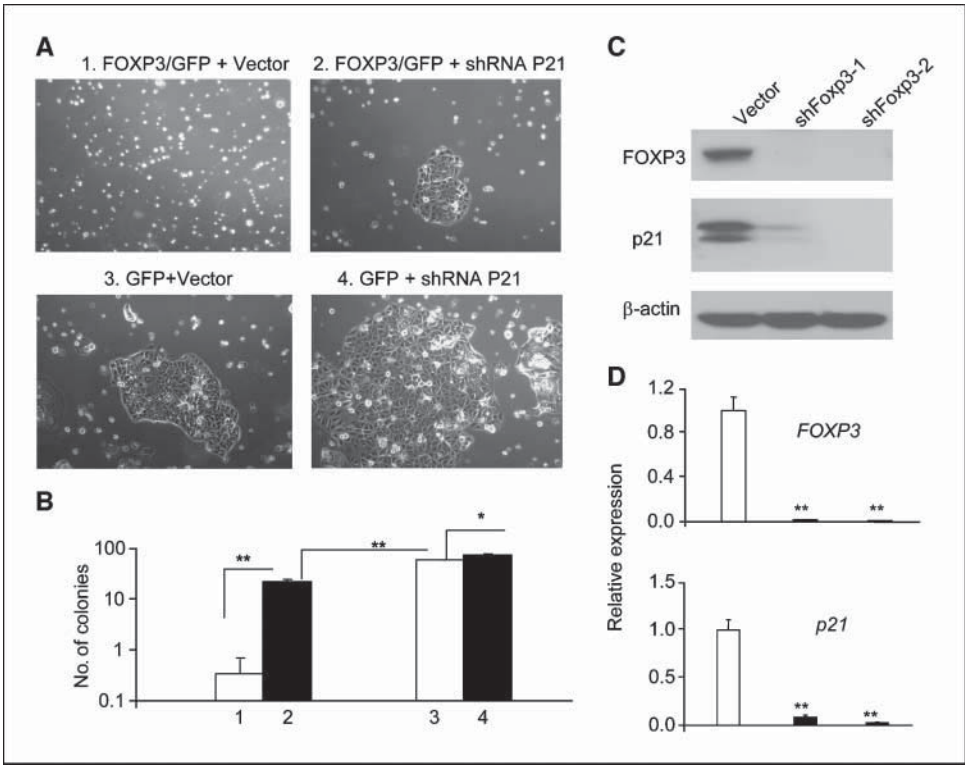

Figure 2. *p21* induction is an underlying mechanism for the tumor suppressor activity of FOXP3. *A,* MCF-7 cells with inducible expression of either FOXP3 (*1* and *2*) or GFP (*3* and *4*) were supertransfected with either vector control (*1* and *3*) or *p21* shRNA (*2* and *4*). After removing untransfected cells by drug selection, the cultures were maintained in doxycyclin-free conditions for 10 d. Photographs of viable (*2–4*) and apoptotic MCF-7 cells (*1*). Magnification, 100×. *B,* the colony number per 60-mm^2 plate. *Columns,* mean of triplicates and representative of three independent experiments; *bars,* SD. *C* and *D,* silencing of *FOXP3* resulted in down-regulation of p21 protein (*C*) and *p21* mRNA (*D*) in human mammary epithelial cell line MCF10A. MCF10A was transfected with either control vector or *FOXP3* shRNAs. The untransfected cells were removed by selection with puromycin. At 2 wk after transfection, the protein levels were determined by Western blotting, using specific anti-FOXP3, anti-p21, and β-actin antibodies as loading control. The mRNA levels of the *FOXP3* and *p21* transcripts were quantitated by real-time PCR. The RNA inputs were normalized against the housekeeping gene *GAPDH*. The vector control was defined as 1.0. *Columns,* mean of triplicates and representative of three independent experiments; *bars,* SD.

p21 as the prototype to study the mechanism by which FOXP3 activates tumor suppressors as the relevance of defective *p21* in breast cancer is well established. In addition, real-time PCR showed induction of *p18* is <2-fold (data not shown). We first used real-time PCR and Western blot to confirm the induction of *p21* after the inducible expression of FOXP3. As shown in Fig. 1*B*, *p21* transcripts were induced by 7-fold in the MCF-7-pBI-FOXP3/green fluorescent protein (GFP) cell line after removal of doxycyclin, but not the MCF-7-pBI-GFP/control cell line under the same culture condition. Western blot analysis confirmed that accumulation of p21 protein followed that of FOXP3 (Fig. 1*C*). To determine whether induction of *p21* contributed to tumor suppression, we transfected the MCF-7 cell lines with either control vector or *p21* shRNA. The transfectants were cultured in the absence of doxycyclin for 10 days and were stained by crystal violets. As shown in Fig. 2*B*, *p21* shRNA specifically increased the number of colonies in the cell line that expressed FOXP3, but barely so for those that expressed GFP. Microscopically, the sizes of colonies were usually larger in the shRNA group, even for those that expressed GFP only, consistent with the notion that endogenous *p21* in the MCF-7 cells limited its growth potential (Fig. 2*A*). Even in the *p21*-silenced group, FOXP3 transfection still reduces the number of colonies by nearly 60%, which is consistent with the contribution of other FOXP3 targets, including those that we have reported recently (22, 23). Nevertheless, the partial restoration of the colonies indicated that *p21* induction contributes to the tumor suppressor activity of the *FOXP3* gene.

FOXP3 maintains p21 levels in normal mammary epithelial cells. An important issue is whether FOXP3 expression contributes to expression of p21 in normal mammary epithelial cells. As shown in Fig. 2*C*, the FOXP3 protein can be identified by Western blot in immortalized human mammary epithelial cell line MCF-10A. To determine the role of *FOXP3* in *p21* expression, we used *FOXP3* shRNA to silence *FOXP3* expression and measured the levels of *p21*

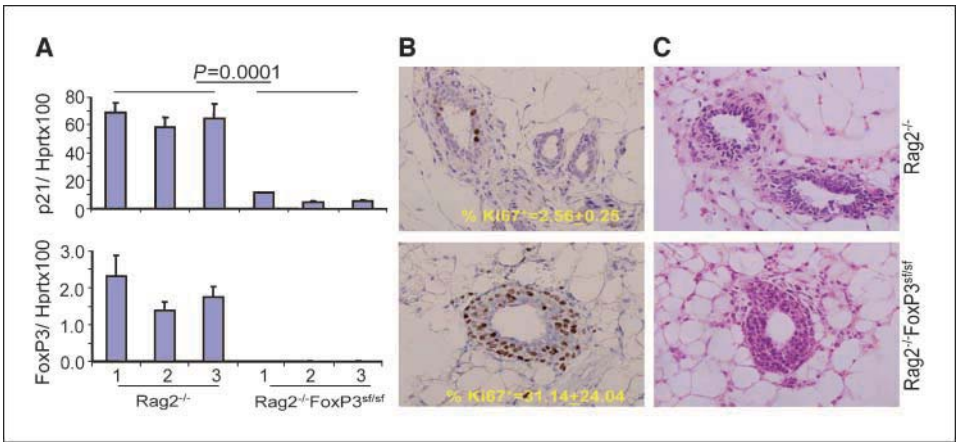

Figure 3. *FoxP3* mutation in benign mammary epithelia increased *p21* transcripts and increased proliferation of epithelial cells. *A, FoxP3* mutation increased *p21* transcripts. Mammary epithelia from virgin *Rag2*$^{-/-}$ *FoxP3*$^{+/+}$ and *Rag2*$^{-/-}$ *FoxP3*$^{sf/sf}$ BALB/c mice were isolated by microdissection. The *p21* and *FoxP3* transcripts were measured by real-time PCR. *Columns,* mean of percentage of housekeeping gene *Hprt*; *bars,* SE. Three independent mice were used in each group. *B,* increased proliferation of the mammary epithelial cells as revealed by Ki67 staining. Representative fields from each group. The means and SDs from groups of three mice are shown in the insert ($P < 0.05$). *C,* H&E staining of 2-month-old virgin *Rag2*$^{-/-}$ *FoxP3*$^{+/+}$ and *Rag2*$^{-/-}$ *FoxP3*$^{sf/sf}$ BALB/c mice. Representative of three mice per group.

transcripts. As shown in Fig. 2*D*, *FOXP3* silencing caused a 5-fold to 10-fold reduction of the *p21* transcripts, which revealed a critical role for *FOXP3* in maintaining *p21* expression in mammary epithelial cells. A similar effect was observed when *FOXP3* was silenced in the early passage of primary human mammary epithelial culture (Supplementary Fig. S1).

To test the role of *FoxP3* in *p21* expression *in vivo*, we microdissected mammary epithelium from 2-month-old $Rag2^{-/-}FoxP3^{sf/sf}$ and $Rag2^{-/-}FoxP3^{+/+}$ mice. The amounts of *p21* transcripts were determined by real-time PCR. As shown in Fig. 3*A*, the *FoxP3* mutation caused ~6-fold reduction in *p21* transcripts. Perhaps due to nonmediated decay caused by frameshift mutation, mammary epithelia from *FoxP3* mutant mice lacked *FoxP3* transcripts. Correspondingly, dramatically increased numbers of breast epithelial cells in the $Rag2^{-/-}FoxP3^{sf/sf}$ mice have entered the cell cycle, as judged by Ki67 staining (Fig. 3*B*). H&E staining of the mammary tissue indicated extensive ductal hyperplasia in the $Rag2^{-/-}FoxP3^{sf/sf}$ mice (Fig. 3*C*). These data showed that the *FoxP3* mutation leads to reduced p21 expression and increased proliferation of normal epithelium *in vivo*. Because the young mice had yet to develop mammary tumor at this age, down-regulation of *p21* is not due to the secondary effect of malignant transformation.

Correlation between expressions of FOXP3 and p21 in human breast cancer. The majority of breast cancer samples lack p21 and FOXP3 expression (5–7, 22, 23). An important issue is, therefore, whether the expression of the two genes is interrelated among human breast cancer samples. To address this issue, we analyzed 62 cases of breast cancer samples in TMA for expression of FOXP3. As shown in Fig. 4, among the $FOXP3^+$ samples, 66% are also $p21^+$. In contrast, only 30% of the $FOXP3^-$ samples expressed p21. The strong correlation between FOXP3 and p21 expression suggests that FOXP3 down-regulation may be an important factor for the lack of p21 among breast cancer tissue.

Specific binding of FOXP3 to the *p21* locus is essential for activation of *p21*. Two *p21* mRNA isoforms (1, NM_078467 and 2, NM_000389) have been reported with different exon 1–exon 2 junctions. To properly align the genomic structure of the locus, we sequenced the *p21* RNA from the MCF-7 cells after the induction of FOXP3. As shown in Supplementary Fig. S2, only isoform 2 was produced in FOXP3-transfected MCF-7 cells. This allowed us to assign the position of intron 1 for the *p21* locus. As illustrated in Fig. 5*A* (*top*), a large number of forkhead binding motifs RYMAAYA (29, 30) and TRTKTRC (refs. 31, 32; R = A, G; M = A, C; Y = C, T; K = G, T) can be identified throughout the *p21* gene. To identify the sites that bind to FOXP3, we induced *FOXP3* by culturing the cell line in the absence of doxycyclin and then used ChIP to determine whether FOXP3 interact with the *p21* locus. To normalize the efficiency of PCR primers, the products were compared with input DNA amplified by the same primers. As shown in Fig. 5*A* (*middle*), quantitative analysis show that peak binding activity localized at the forkhead/HNF-3 binding motif at 0.2 kb 3′ of TSS. Low but detectable levels of DNA are observed over an 8-kb fragment, which could be due to either the low resolution of ChIP or the existence of multiple weaker binding sites. To confirm the specific requirement for FOXP3 for the signal at 0.2 kb, we also compared the signal to uninduced pBI-FOXP3/GFP cell lines and pBI-GFP control cell lines cultured in the presence or absence of doxycyclin. As shown in Fig. 5*A* (*bottom*), the *p21* region is precipitated if, and only if, FOXP3 was induced.

To directly show the function and specificity of the *FOXP3*-mediated induction of *p21*, we first produced three constructs consisting of overlapping fragments of the 5′ of the *p21* locus

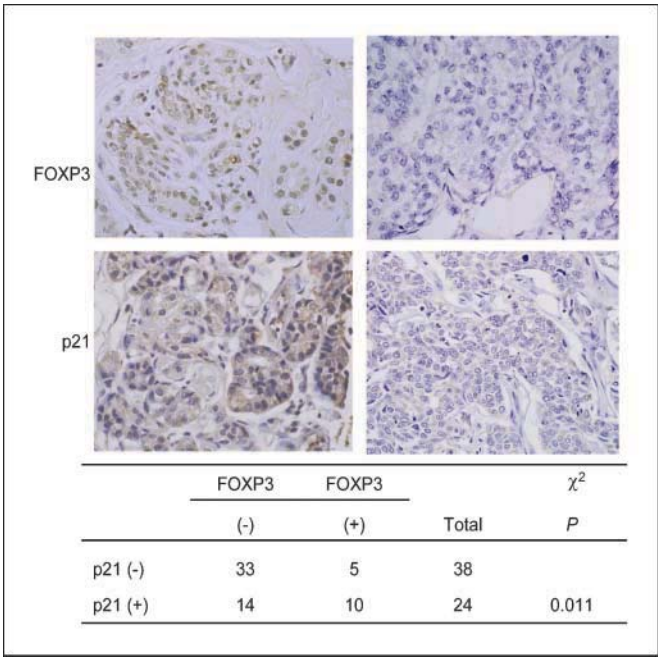

	FOXP3 (-)	FOXP3 (+)	Total	χ^2 *P*
p21 (-)	33	5	38	
p21 (+)	14	10	24	0.011

Figure 4. A positive correlation between FOXP3 and p21 expression in human breast cancer. Tissue microarray samples were stained with either anti-FOXP3 antibody or anti-p21 antibody and scored by a double-blind fashion. Samples with nuclear staining by the anti-FOXP3 antibody were scored as positive. Samples with >10% p21 staining in nuclear and/or cytosolic were scored as positive. Magnification, 600×. *Bottom,* summary data from 62 independent cases. The *P* value of the χ^2 test is listed.

(Fig. 5*B*). Using a dual-luciferase assay, we found that FOXP3-mediated induction of *p21* requires sequences that are both 5′ and 3′ to TSS, with the maximal activity requiring −540 and +365 bp at 5′ and 3′, respectively. Further extension at 3′ significantly reduced the *p21* induction (Fig. 5*B*). We, therefore, used the optimal reporter to confirm the function of the forkhead binding site at the 0.2 kb at 3′ of TSS. As shown in Fig. 5*C*, whereas wild-type (WT) reporter is induced by FOXP3 expression, mutation of the forkhead binding site abrogated induction. These data showed that the specific *cis*-element is essential for FOXP3-mediated activation of *p21* locus.

It has been shown that c-Myc can target the *p21* promoter and inhibit its expression (33–35). To determine whether the *FOXP3* gene regulates *p21* directly, we measured the effects of FOXP3 on the *p21* promoter activity in the *c-Myc* knockout cell line. As shown in Fig. 5*D*, the promoter activity of *p21* was significantly induced by FOXP3 in *c-Myc* knockout cells. The relatively low induction, compared with HEK 293 cells, is likely due to the drastically reduced transfection efficiency of the Myc-deficient cell line.[4]

Localized chromatin modification as a mechanism for FOXP3-induced expression of *p21*. Recent studies showed that FOXP3-mediated induction of gene expression is associated with histone acetylation (36). We, therefore, used anti–acetyl-H3 antibodies to monitor local chromatin changes associated with FOXP3 binding. As shown in Fig. 6*A* and *B*, in cells expressing FOXP3, H3 acetylation in the +0.2-kb site of *p21* was increased by >2-fold. The increase in the neighboring areas mirrored what was observed with FOXP3 binding. These data showed that FOXP3 enhances the H3 acetylation of *p21*, especially at the 0.2-kb region. We carried out

[4] Our unpublished observation.

ChIP analysis using antibodies specific for HDAC1 to HDAC7. The MCF-7 cells with or without FOXP3 induction were compared. As shown in Fig. 6*B*, a generalized reduction of HDAC association to the *p21* locus was observed after FOXP3 induction. However, by far, the strongest effect was observed at the 0.2-kb site, wherein FOXP3 associates with the *p21* locus. Moreover, although a reduction of HDAC1 to HDAC7 was observed after FOXP3 binding, the most significant reduction was observed on HDAC2 and HDAC4, as these two HDACs showed the strongest association before FOXP3 induction.

To determine whether HDAC2 and HDAC4 are involved in *p21* up-regulation, we used shRNAs to modulate their expression. As shown in Fig. 6*C*, two independent shRNAs were specifically silencing the expression of either HDAC2 or HDAC4. Correspondingly, the levels of *p21* transcripts were increased by 2-fold to 3-fold after the silence of either gene. Note that some of the p21 protein induced by *HDAC* shRNAs had a molecular weight of 15 kDa rather than 21 kDa. This is likely due to the cleavage of p21 associated with a general increase in histone acetylation, as reported by others (37). To test if HDAC2 and HDAC4 are necessary mediators of *p21* induction by FOXP3, we transfected FOXP3 into MCF-7 cells, in which HDAC2 and HDAC4 are silenced, and compared the levels of *p21* in either FOXP3-tracnsfected or vector control–transfected cells. As shown in Fig. 6*C*, FOXP3-mediated induction of *p21* is abrogated in the HDAC4-silenced cell lines. These data further support the notion that FOXP3-mediated induction of p21 is

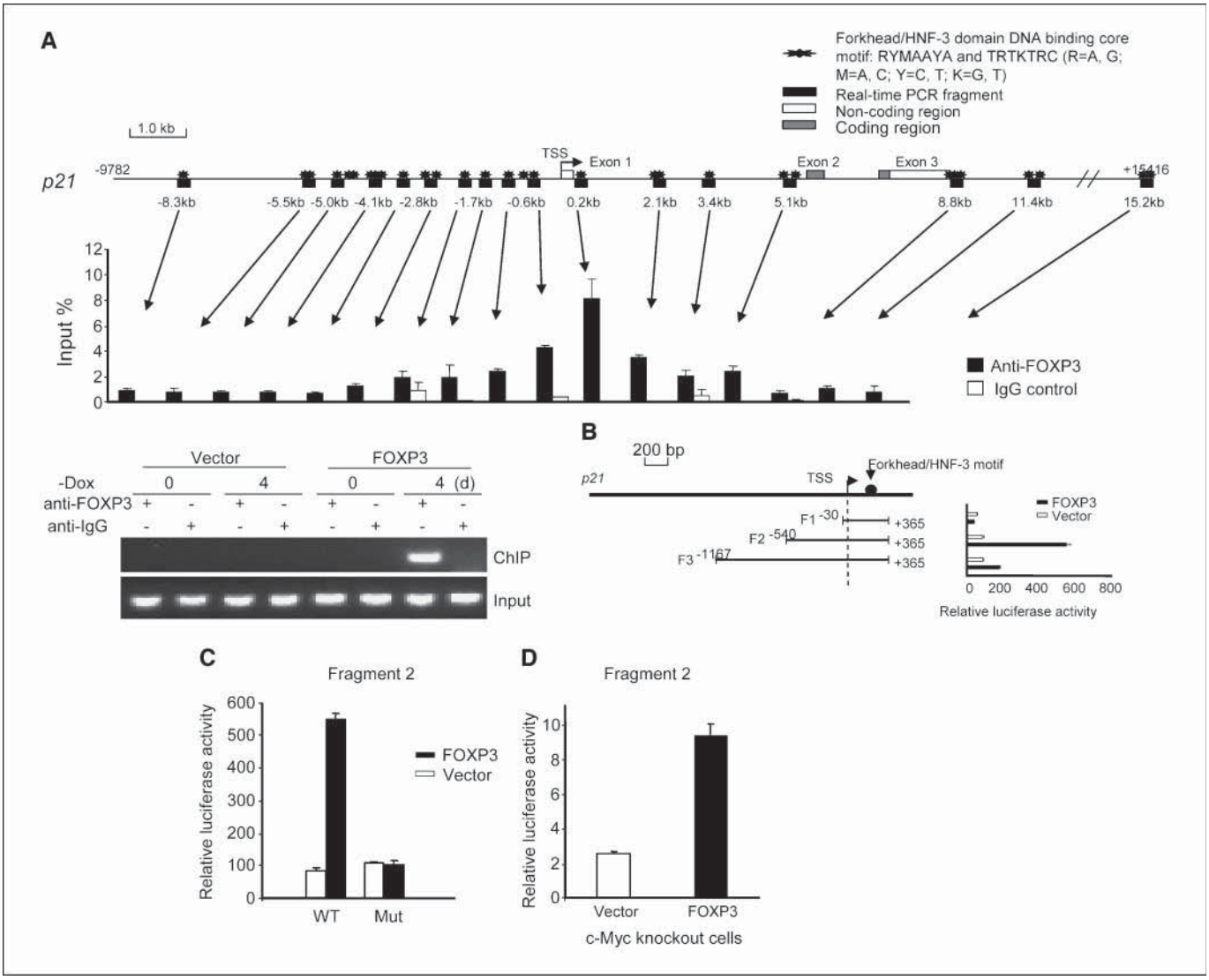

Figure 5. FOXP3 as a transcription activator for *p21. A,* ChIP. *Top,* a diagram of the *p21* gene, including the promoter and exon 1 to 3 (NM_000389). *Black asterisks,* forkhead binding motifs; *black columns,* regions surveyed by real-time PCR. *Middle,* amount of DNA precipitated by either control IgG or anti-FOXP3 monoclonal antibody expressed as percentage of the total input genomic DNA. *Columns,* means of triplicates; *bars,* SD. This experiment has been repeated twice with similar results. *Bottom,* specificity of the ChIP assay, as shown by the requirements for both FOXP3 induction and anti-FOXP3 antibody. *B,* identification of the promoter region most responsive to FOXP3-mediated induction. The HEK293 cells were transfected with either vector control or *FOXP3* (1 μg/well) in conjunction with the luciferase reporter driven by different 5′ promoter regions of the *p21* gene (0.5 μg/well). pRL-TK was used as internal control. The luciferase activity from the cells transfected with the pGL2 basic vector was arbitrarily defined as 1.0. *Columns,* means of triplicates repeated at least thrice; *bars,* SD. *C,* site-directed mutagenesis of one candidate forkhead/HNF-3 binding motif in the p21 promoter abrogated the induction of the *p21* transcription activity by FOXP3. The WT forkhead-binding motif TGTGTGC was mutated into CCCAAAA. The promoter activity was measured and normalized as detailed in *B. Columns,* means of triplicates; *bars,* SD. This experiment has been repeated twice with similar results. *D, p21* transcription is directly induced by FOXP3 by a *c-Myc*–independent mechanism. Transfection of *FOXP3* into *c-Myc*$^{-/-}$ cells increased *p21* activity, as by a luciferase assay. *Columns,* means of triplicates; *bars,* SD. This experiment has been repeated thrice.

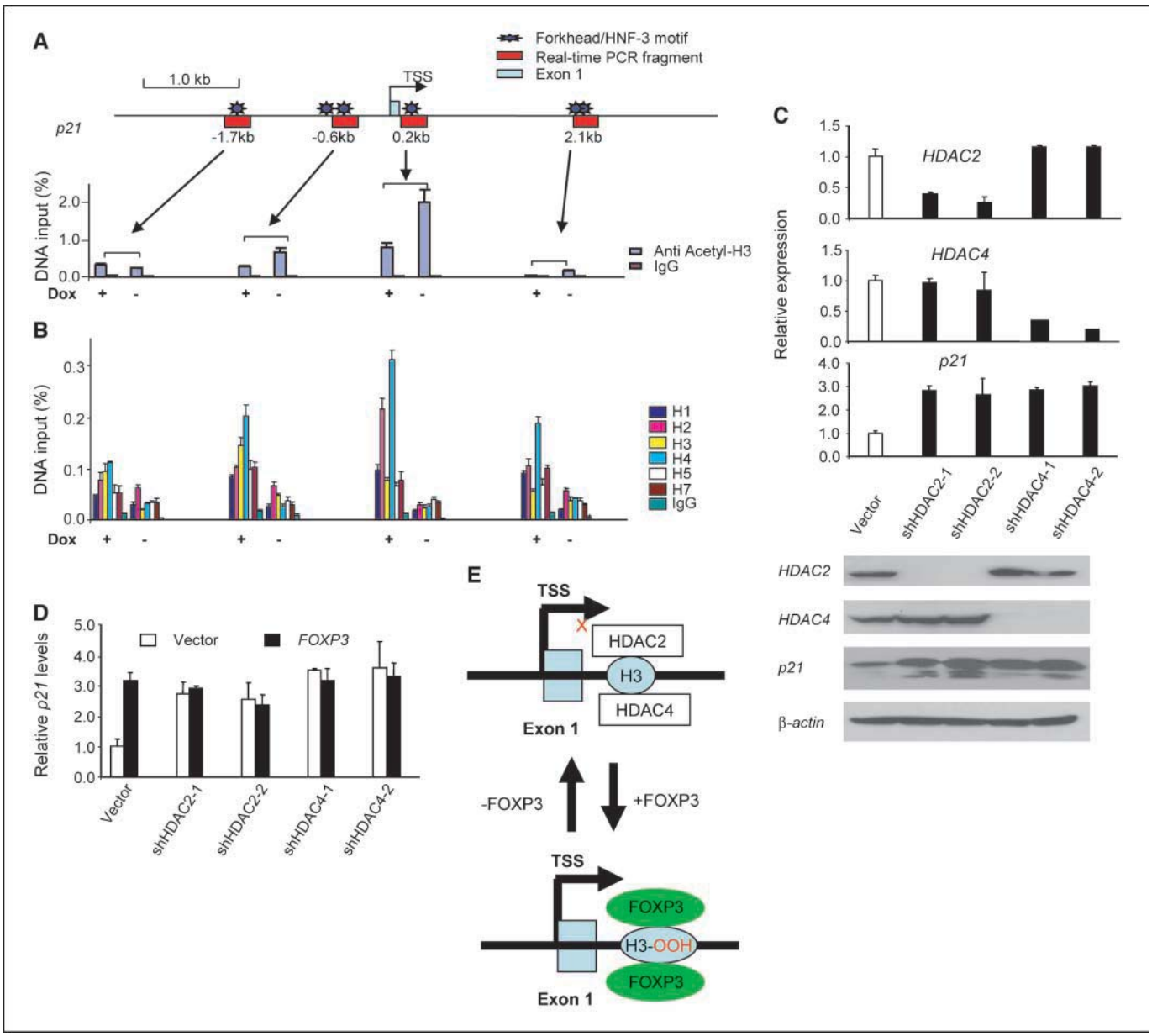

Figure 6. *A,* FOXP3 specifically increased acetylation of histone H3 associated with the FOXP3 binding site by inhibiting association of HDAC 2 and 4. FOXP3 increases acetylation of histone H3 associated with the *FOXP3* binding site. *B,* the increased acetylation of H3 is due to FOXP3-mediated inhibition association of HDAC2 and HDAC4 to the site. The MCF-7 cells with inducible FOXP3 expression were cultured with (−*FOXP3*) or without (+*FOXP3*) doxycyclin for 4 d and subjected to ChIP analysis using acetyl-H3 (*A*) and HDAC1, HDAC2, HDAC3, HDAC4, HDAC5, and HDAC7 (*B*) antibody or control IgG. Precipitated genomic DNA was probed for the promoter/enhancer regions of the *p21* locus by real-time PCR. The amounts of DNA precipitated were expressed as percentage of the total input genomic DNA. *Columns,* means of triplicates; *bars,* SD. Representative of three separate experiments. *C,* shRNA silencing of either *HDAC2* or *HDAC4* is sufficient to induce *p21* expression. Data in bar graphs are from real-time PCR quantitation of shRNA efficacy and the effect of shRNA silencing using the means of the vector group as 1.0. *Bottom,* Western blotting. Note that some p21 proteins in *HDAC4* or *HDAC2* shRNA groups are degraded products with a molecular weight of 15 kDa whereas those in the control group consisted of mostly intact p21. These experiments have been repeated four times with similar results. *D,* silencing HDAC4 abrogates induction of *p21* by FOXP3. Control or HDAC2/HDAC4-silenced MCF-7 cells were transfected with *FOXP3* cDNA. After removal of nontransfected cells by blasticidin, the levels of *p21* transcripts were determined by real-time PCR. Data have been repeated twice. *E,* diagram of a proposed mechanism of FOXP3-mediated gene activation. FOXP3 removes association of HDAC2 and HDAC4 and, thereby, increases H3 acetylation and gene activation.

mediated by the disruption of HDAC2-mediated and HDAC4-mediated repression.

Discussion

Mechanism of *p21* regulation in normal and cancerous epithelial cells may hold the keys to the molecular mechanism of carcinogenesis. Here, we present several lines of evidence demonstrating a critical role of *p21* as a downstream target of FOXP3, and its expression contributes to the FOXP3-mediated growth inhibition of a breast cancer cell line.

First, in confirming the cDNA microarray data, we showed that inducible expression of *FOXP3* induced the *p21* transcripts and protein in breast cancer cell line MCF-7. The induction is mediated by transcription regulation, as it is reflected in luciferase assay. ChIP analysis revealed that a specific site at 0.2 kb downstream of

TSS is necessary for FOXP3-mediated induction by FOXP3. Moreover, the induction is not an artifact of *FOXP3* overexpression, as shRNA silencing of the *FOXP3* gene leads to a dramatic reduction of *p21* in primary mammary epithelial cells.

Second, to determine whether induction of *p21* contributes to growth inhibition of the tumor cell line, we tested whether blunting *p21* induction by shRNA abrogate growth inhibition by FOXP3. Our data showed the significant, albeit incomplete, rescue of FOXP3-mediated growth inhibition. The significant rescue shows an important role of *p21* induction in FOXP3-mediated growth inhibition in MCF-7 cell line. Other recent studies indicate that FOXP3 also inhibits growth by repressing the expression of *HER-2* and *SKP2* (22, 23). Thus, depending on tumor cell lines used, FOXP3-mediated inhibition of oncogenes and induction of tumor suppressor may work either independently or in concert to cause growth inhibition of breast cancer cell line.

Third, our analysis of 62 cases of breast cancer samples showed a significant correlation between expression of FOXP3 and p21. Nevertheless, not unlike other tumor suppressor targets, there was no 1:1 correlation between expression of FOXP3 and p21. For instance, ~30% of cases that stained positive for FOXP3 still lack detectable p21. This is, in part, due to the fact that nearly one third of breast cancer samples show somatic missense mutation of *FOXP3* (22, 23). Conversely, nearly one third of the FOXP3 negative tumor cells still express *p21*. This can be due to either the false-negative staining of FOXP3, perhaps relating to the quality of tumor tissues, or the levels of FOXP3 expression in the first place. In addition, because p53 can induce *p21* expression, it is possible that the p21 expression in FOXP3-negative tumor samples was due to functional p53. The limited sample set used in this study cannot distinguish these possibilities. Regardless of how the discrepancies are explained, the positive association between p21 and FOXP3 in clinical samples, when viewed in the context of the data in mice with *FoxP3* mutation and the *in vitro* analysis of normal and malignant tumor cells, made a compelling case that *FOXP3* is a major regulator for *p21* expression in breast cancer. Recent studies revealed an interesting role of *p21* loss and tamoxifen-stimulated growth of breast cancer (9). It is of great interest to determine whether genetic lesion to *FOXP3* may account for the p21 loss and, therefore, the unusual response to a widely used drug.

Finally, whereas a number of studies have addressed the mechanism of FOXP3-mediated gene repression, the mechanism by which FOXP3 directly induces gene expression remained largely obscure. A recent report showed association between FOXP3-induced gene activation and histone acetylation (36), although the mechanism and significance of such acetylation have not been addressed. Our data showed that FOXP3 binding to a specific site in intron 1 of *p21* increased histone H3 acetylation by reducing binding of HDAC4 and HDAC2 to the same site (Fig. 6*E*). Gene silencing with shRNA confirmed the significance of these two HDACs in *p21* expression, although FOXP3 did not repress expression of either HDAC2 or HDAC4 (Supplementary Fig. S4). Therefore, our data provide a novel mechanism for FOXP3-mediated transcription activation. Because FOXP3 has been shown to recruit histone acetyl transferases (38), it is of interest to investigate whether this interaction contributes, either directly or indirectly, to increased H3 acetylation in the *p21* locus.

Taken together, our data showed *p21* as a downstream target for FOXP3, the first X-linked tumor suppressor in breast cancer. Because *p21* serves as an important target for all major tumor suppressor genes of breast cancer and because irreversible genetic lesion to *p21* is relatively rare, it might be possible to reactivate *p21* in cancer by inducing FOXP3. Whereas *p21* induction can be achieved by a general silencing of HDAC2 and HDAC4, the induced *p21* are rapidly degraded, presumably due to the simultaneous induction of other proteins involved in p21 cleavage (37). On the other hand, our data showed that *p21* induced by FOXP3 remained intact and mediates tumor suppression. Therefore, reactivating FOXP3 may prove to be a more relevant approach.

Disclosure of Potential Conflicts of Interest

No potential conflicts of interest were disclosed.

Acknowledgments

Received 9/29/2008; revised 12/19/2008; accepted 1/7/2009; published OnlineFirst 3/10/09.

Grant support: NIH grant CA120910 (Y. Liu), Department of Defense grant W81XWH08-1-0537 (Y. Liu), and American Cancer Society grant RSG-06-072-01-TBE (P. Zheng).

The costs of publication of this article were defrayed in part by the payment of page charges. This article must therefore be hereby marked *advertisement* in accordance with 18 U.S.C. Section 1734 solely to indicate this fact.

References

1. el-Deiry WS, Tokino T, Velculescu VE, et al. WAF1, a potential mediator of p53 tumor suppression. Cell 1993; 75:817–25.
2. Gu Y, Turck CW, Morgan DO. Inhibition of CDK2 activity *in vivo* by an associated 20K regulatory subunit. Nature 1993;366:707–10.
3. Harper JW, Adami GR, Wei N, Keyomarsi K, Elledge SJ. The p21 Cdk-interacting protein Cip1 is a potent inhibitor of G_1 cyclin-dependent kinases. Cell 1993;75: 805–16.
4. Xiong Y, Hannon GJ, Zhang H, Casso D, Kobayashi R, Beach D. p21 is a universal inhibitor of cyclin kinases. Nature 1993;366:701–4.
5. Pellikainen MJ, Pekola TT, Ropponen KM, et al. p21WAF1 expression in invasive breast cancer and its association with p53, AP-2, cell proliferation, and prognosis. J Clin Pathol 2003;56:214–20.
6. Pinto AE, Andre S, Laranjeira C, Soares J. Correlations of cell cycle regulators (p53, p21, pRb and mdm2) and c-erbB-2 with biological markers of proliferation and overall survival in breast cancer. Pathology (Phila) 2005; 37:45–50.
7. Tiezzi DG, Andrade JM, Ribeiro-Silva A, Zola FE, Marana HR, Tiezzi MG. HER-2, p53, p21 and hormonal receptors proteins expression as predictive factors of response and prognosis in locally advanced breast cancer treated with neoadjuvant docetaxel plus epirubicin combination. BMC Cancer 2007;7:36.
8. Rowland BD, Bernards R, Peeper DS. The KLF4 tumour suppressor is a transcriptional repressor of p53 that acts as a context-dependent oncogene. Nat Cell Biol 2005;7:1074–82.
9. Abukhdeir AM, Vitolo MI, Argani P, et al. Tamoxifen-stimulated growth of breast cancer due to p21 loss. Proc Natl Acad Sci U S A 2008;105:288–93.
10. Shiohara M, el-Deiry WS, Wada M, et al. Absence of WAF1 mutations in a variety of human malignancies. Blood 1994;84:3781–4.
11. Dulic V, Kaufmann WK, Wilson SJ, et al. p53-dependent inhibition of cyclin-dependent kinase activities in human fibroblasts during radiation-induced G_1 arrest. Cell 1994;76:1013–23.
12. Slebos RJ, Lee MH, Plunkett BS, et al. p53-dependent G_1 arrest involves pRB-related proteins and is disrupted by the human papillomavirus 16 E7 oncoprotein. Proc Natl Acad Sci U S A 1994;91:5320–4.
13. Somasundaram K, Zhang H, Zeng YX, et al. Arrest of the cell cycle by the tumour-suppressor BRCA1 requires the CDK-inhibitor p21WAF1/CiP1. Nature 1997;389:187–90.
14. Aliouat-Denis CM, Dendouga N, Van den Wyngaert I, et al. p53-independent regulation of p21Waf1/Cip1 expression and senescence by Chk2. Mol Cancer Res 2005;3:627–34.
15. Chen X, Johns DC, Geiman DE, et al. Kruppel-like factor 4 (gut-enriched Kruppel-like factor) inhibits cell proliferation by blocking G_1-S progression of the cell cycle. J Biol Chem 2001;276:30423–8.
16. Zhang W, Geiman DE, Shields JM, et al. The gut-enriched Kruppel-like factor (Kruppel-like factor 4) mediates the transactivating effect of p53 on the p21WAF1/Cip1 promoter. J Biol Chem 2000;275:18391–8.
17. Narla G, Heath KE, Reeves HL, et al. KLF6, a candidate tumor suppressor gene mutated in prostate cancer. Science 2001;294:2563–6.

18. Duan Z, Zarebski A, Montoya-Durango D, Grimes HL, Horwitz M. Gfi1 coordinates epigenetic repression of p21Cip/WAF1 by recruitment of histone lysine methyltransferase G9a and histone deacetylase 1. Mol Cell Biol 2005;25:10338–51.
19. Lagger G, Doetzlhofer A, Schuettengruber B, et al. The tumor suppressor p53 and histone deacetylase 1 are antagonistic regulators of the cyclin-dependent kinase inhibitor p21/WAF1/CIP1 gene. Mol Cell Biol 2003;23: 2669–79.
20. Richon VM, Sandhoff TW, Rifkind RA, Marks PA. Histone deacetylase inhibitor selectively induces p21WAF1 expression and gene-associated histone acetylation. Proc Natl Acad Sci U S A 2000;97:10014–9.
21. Xia W, Nagase S, Montia AG, et al. BAF180 is a critical regulator of p21 induction and a tumor suppressor mutated in breast cancer. Cancer Res 2008;68:1667–74.
22. Zuo T, Wang L, Morrison C, et al. FOXP3 is an X-linked breast cancer suppressor gene and an important repressor of the HER-2/ErbB2 oncogene. Cell 2007;129: 1275–86.
23. Zuo T, Liu R, Zhang H, et al. FOXP3 is a novel transcriptional repressor for the breast cancer oncogene SKP2. J Clin Invest 2007;117:3765–73.
24. Chang X, Gao JX, Jiang Q, et al. The Scurfy mutation of FoxP3 in the thymus stroma leads to defective thymopoiesis. J Exp Med 2005;202:1141–51.
25. Prouty SM, Hanson KD, Boyle AL, et al. A cell culture model system for genetic analyses of the cell cycle by targeted homologous recombination. Oncogene 1993;8: 899–907.
26. Mateyak MK, Obaya AJ, Adachi S, Sedivy JM. Phenotypes of c-Myc-deficient rat fibroblasts isolated by targeted homologous recombination. Cell Growth Differ 1997;8:1039–48.
27. Dai M, Wang P, Boyd AD, et al. Evolving gene/transcript definitions significantly alter the interpretation of GeneChip data. Nucleic Acids Res 2005;33:e175.
28. Im H, Grass JA, Johnson KD, Boyer ME, Wu J, Bresnick EH. Measurement of protein-DNA interactions *in vivo* by chromatin immunoprecipitation. Methods Mol Biol 2004;284:129–46.
29. Harbison CT, Gordon DB, Lee TI, et al. Transcriptional regulatory code of a eukaryotic genome. Nature 2004;431:99–104.
30. Pic A, Lim FL, Ross SJ, et al. The forkhead protein Fkh2 is a component of the yeast cell cycle transcription factor SFF. EMBO J 2000;19:3750–61.
31. Cardinaux JR, Chapel S, Wahli W. Complex organization of CTF/NF-I, C/EBP, and HNF3 binding sites within the promoter of the liver-specific vitellogenin gene. J Biol Chem 1994;269:32947–56.
32. Kaufmann E, Knochel W. Five years on the wings of fork head. Mech Dev 1996;57:3–20.
33. Seoane J, Le HV, Massague J. Myc suppression of the p21(Cip1) Cdk inhibitor influences the outcome of the p53 response to DNA damage. Nature 2002;419: 729–34.
34. Mitchell KO, El-Deiry WS. Overexpression of c-Myc inhibits p21WAF1/CIP1 expression and induces S-phase entry in 12-O-tetradecanoylphorbol-13-acetate (TPA)-sensitive human cancer cells. Cell Growth Differ 1999;10: 223–30.
35. Claassen GF, Hann SR. A role for transcriptional repression of p21CIP1 by c-Myc in overcoming transforming growth factor β-induced cell-cycle arrest. Proc Natl Acad Sci U S A 2000;97:9498–503.
36. Chen C, Rowell EA, Thomas RM, Hancock WW, Wells AD. Transcriptional regulation by Foxp3 is associated with direct promoter occupancy and modulation of histone acetylation. J Biol Chem 2006; 281:36828–34.
37. Chai F, Evdokiou A, Young GP, Zalewski PD. Involvement of p21(Waf1/Cip1) and its cleavage by DEVD-caspase during apoptosis of colorectal cancer cells induced by butyrate. Carcinogenesis 2000; 21:7–14.
38. Samanta A, Li B, Song X, et al. TGF-β and IL-6 signals modulate chromatin binding and promoter occupancy by acetylated FOXP3. Proc Natl Acad Sci U S A 2008;105: 14023–7.

Molecular Biology, Pathobiology, and Genetics

Activating Transcription Factor 2 and c-Jun–Mediated Induction of FoxP3 for Experimental Therapy of Mammary Tumor in the Mouse

Yan Liu,[1] Yin Wang,[1] Weiquan Li,[1] Pan Zheng,[1,2] and Yang Liu[1,3]

[1]Division of Immunotherapy, Department of Surgery, Section of General Surgery, and Comprehensive Cancer Center; [2]Department of Pathology; and [3]Division of Molecular Medicine and Genetics, Department of Medicine, University of Michigan, Ann Arbor, Michigan

Abstract

***FOXP3* is inactivated in breast cancer cells by a number of mechanisms, including somatic mutations, deletion, and epigenetic silencing. Because the mutation and deletion are usually heterozygous in the cancer samples, it is of interest to determine whether the gene can be induced for the purpose of cancer therapy. Here, we report that anisomycin, a potent activator of activating transcription factor (ATF) 2, and c-Jun-NH_2-kinase, induces expression of *FoxP3* in both normal and malignant mammary epithelial cells. The induction is mediated by ATF2 and c-Jun. Targeted mutation of *ATF2* abrogates both constitutive and inducible expression of *FoxP3* in normal epithelial cells. Both ATF2 and c-Jun interact with a novel enhancer in the intron 1 of the *FoxP3* locus. Moreover, shRNA silencing of *ATF2* and *FoxP3* reveals an important role of ATF2-FoxP3 pathway in the anisomycin-induced apoptosis of breast cancer cells. A low dose of anisomycin was also remarkably effective in treating established mammary tumor in the mice. Our data showed that *FoxP3* can be reactivated for cancer therapy.** [Cancer Res 2009;69(14):5954–60]

Introduction

The overwhelming majority of tumor suppressor genes are autosomal, and their inactivations involve two genetic events (1–4). The best defined two hits of the tumor suppressors in cancer cells are usually irreversible, such as deletion or mutations (3, 4). More recently, however, it has become increasingly clear that epigenetic inactivation of tumor suppressors plays a critical role in inactivating tumor suppressor genes (5). On the other hand, due to X-inactivation, the X-linked tumor suppressor genes are operatively hemizygous, and can be inactivated by a single hit (6). This notion has been substantiated by the recent identification of two tumor suppressor genes, *FoxP3* for breast cancer (7) and *WTX* for Wilms' tumor (8). Because the majority of mutations and/or deletions associated with X-linked tumor suppressor genes are heterozygous (7, 8), most cancer cells have a wild-type (WT) allele that has not been irreversibly inactivated (7).

An important aspect of tumor therapy is how to restore the function of tumor suppressors. For those with two irreversible genetic changes, such as p53, this has been technically challenging, although a pharmaceutical restoration of mutant protein function has been reported (9). Because X-linked tumor suppressor genes are operationally hemizygous, only one allele is subject to genetic selection in cancer cells. The other allele is therefore genetically intact and can potentially be induced to suppress tumor growth. Based on this concept, we searched for a biochemical pathway that can be activated to induce FOXP3 expression in breast cancer cells. Here, we report that anisomycin, which is commonly used to induce stress responses of cells, induces expression of *FOXP3* in breast cancer cell lines. Our biochemical and genetic analyses revealed that activating transcription factor (ATF)*2*, which was recently shown to be a tumor suppressor gene in the mouse (10), is essential for the induction of FoxP3 and FoxP3-mediated apoptosis. Moreover, ATF-2 forms heterodimer with c-Jun to activate transcription of *FoxP3*. These data show a novel function of ATF2 in the expression of *FoxP3* in the epithelial cells and suggest a novel approach for the therapy of breast cancer.

Materials and Methods

Antibodies and reagents. Anti–ATF-2 (20F1), phospho-ATF2-(Thr71), and activated caspase-3 were purchased from Cell Signaling, Inc. Other vendors are as follows: anti-Foxp3 (eBioscience; #14-5779-82); and anti–β-actin (I-19), c-Jun (NX), and phosphor-c-Jun (KM-1; Santa Cruz Biotechnology, Inc.). Chemicals SP600125, SB203580, and PD98059 were purchased from CalBiochem, Inc., whereas anisomycin was purchased from Sigma, Inc.

Experimental animals. Mice heterozygous for *Atf2* null mutation ($Atf2^{tm1Glm}$/$Atf2^{+}$129S2/SvPas; ref. 11) were revived from the frozen embryo bank in The Jackson Laboratory. Heterozygous mice were crossed to produce $Atf2^{+/+}$ and $Atf2^{-/-}$ littermates. BALB/c mice were purchased from Charles River through a National Cancer Institute Subcontract. All studies involving animal has been approved by University Committee on Use and Care of Animals at University of Michigan.

Preparation of mammary epithelial cell culture. Mouse mammary fat pads were removed from 6- to 8-wk-old virgin female mice and minced into small pieces. After collagenase digestion at 37°C in a shaking incubator in DMEM supplemented with 5% FCS, cells were sieved through a 70-μm cell strainer (BD Falcon) to obtain a single-cell suspension. The cells were cultured in DMEM supplemented with 10% fetal bovine serum and 10 ng/mL epithelial growth factor. At day 3 of culture, fibroblast cells were removed by a short digestion with 0.05% trypsin-EDTA as less adherent cells.

Measurement of *FOXP3* transcripts. Total cDNA were prepared from breast cancer cell lines or epithelial cultures. The levels of FOXP3 mRNA were measured by reverse transcription-PCR (RT-PCR) under two conditions. Full-length encoding regions were analyzed by agarose

Note: Supplementary data for this article are available at Cancer Research Online (http://cancerres.aacrjournals.org/).

Y. Liu and Y. Wang contributed equally to the study.

Requests for reprints: Yang Liu or Pan Zheng, University of Michigan, 109 Zina Pitcher Place, Ann Arbor, MI 48109. Phone: 734-615-3158; Fax: 734-763-2162; E-mail: yangl@umich.edu or panz@umich.edu.

doi:10.1158/0008-5472.CAN-09-0778

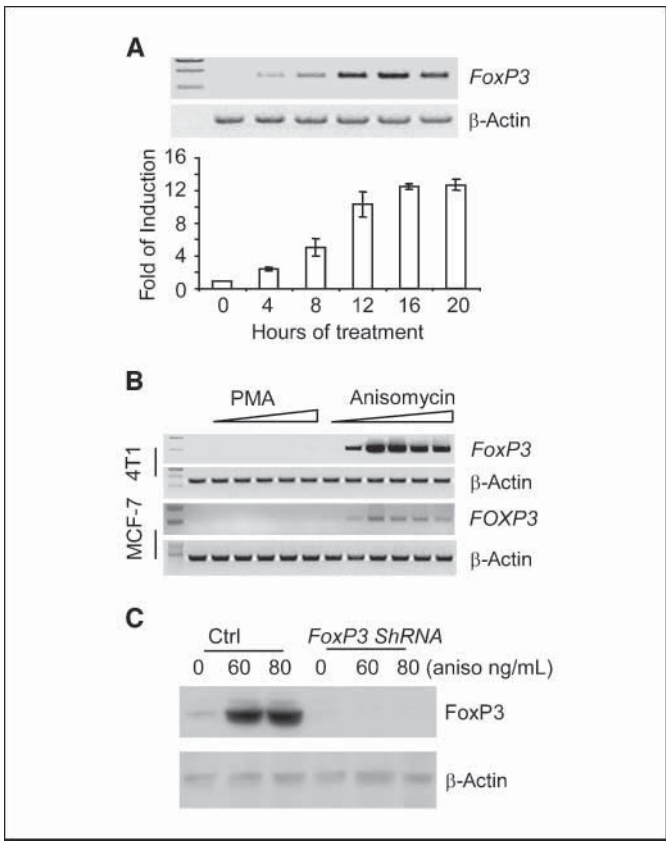

Figure 1. Anisomycin rapidly induces FoxP3 expression in mouse and human breast cancer cell lines. *A,* induction of FoxP3 transcripts by anisomycin (0.1 μg/mL). *Top,* kinetics of *FoxP3* induction in mouse mammary tumor cell line TSA, as measured by RT-PCR for cDNA covering the entire coding region. *Bottom,* the induction of FoxP3 in TSA by real-time PCR. *Columns,* means of three independent experiments; *bars,* SD. The transcript level of 0 h is artificially defined as 1.0. *B,* induction of FoxP3 by anisomycin (0.01, 0.05, 0.1, 0.25, 0.5, 1.0 μg/mL), but not by PMA (0.01, 0.1, 0.5, 1.0, 2.5 μg/mL), in mouse mammary tumor cell line 4T1 or human breast cancer cell line MCF7 by RT-PCR, using primers spanning from start coden to stop coden. *C,* anisomycin induces FoxP3 protein, as revealed by Western blot. The specificity of analysis and dependence of FoxP3 transcript is confirmed by *FoxP3* shRNA. All data are representative of at least three independent experiments.

gel electrophoresis, whereas shorter transcripts were quantitated using real-time PCR. All primers for PCR were listed in Supplementary Table S1.

***ShRNA* lentiviral vector.** The lentivirus-based shRNA expressing vectors were created by introducing the murine U6 RNA polymerase III promoter and a murine phosphoglycerate kinase promoter (pGK)–driven enhanced green fluorescent protein expression cassette into a vector of pLenti6/V5-D-TOPO back bone without cytomegalovirus promoter. Hairpin shRNA sequence of *FoxP3, JNK1, JNK2*, and *Atf2* (*FoxP3*: 5′-aagccatggcaatagttcctt-3′; *FOXP3*: 5′-*gcagcggacactcaatgag*-3′; *JNK12*: 5′-*agaaggtaggacattcctt*-3′ and 5′-*aagcctagtaatatagtagt*-3′; *Atf2*: 5′-*cttctgttgtagaaacaac*-3′ and 5′-*agcacgtaatgacagtgtca*-3′) were cloned into the lentiviral shRNA expressing vectors by restriction sites of *Apa*I and *Eco*RI.

Electrophoresis mobility shift assay. Anisomycin were added to 4T1 cells in conjunction with either vehicle control or kinase inhibitor SP600125 at a dose of 2 μg/mL for 2 h before cells lysed. The nuclear extracts were mixed with either WT or mutant probes in the presence of either control anti–c-Jun (Santa Cruz; sc-45X) or anti-ATF2 (Cell Signaling, #9226) antibodies, as indicated and analyzed by electrophoresis, as described (12).

Western blot. Protein samples for Western blot were prepared by lysing cultured cells in SDS sample buffer, resolved on 10% SDS-PAGE, and electroblotted onto nitrocellulose membranes. Membranes with transferred proteins were incubated with primary antibody followed by incubation with horseradish peroxidase conjugated to the secondary antibody. Chemiluminescence reaction using the enhanced chemiluminescence kit (Amersham Biosciences) was detected by film.

Chromatin immunoprecipitation (ChIP) was carried out according to a published procedure (13). Briefly, the vehicle or 2-h anisomycin-treated 4T1 cells were sonicated and fixed with 1% paraformaldehyde. The anti–phospho-c-Jun or anti–phosphor-ATF2 antibodies or control rabbit IgG were used to pull down chromatin associated with these proteins. The amounts of the specific DNA fragments were quantitated by real-time PCR and normalized against the genomic DNA preparation from the same cells.

Immunoflurensence staining. TSA cells were treated or left untreated with vehicle DMSO or 50 ng/mL of anisomycin for 24 h. After that, the cells were fixed by methanol, permeabilized with 0.3% Triton-X100, and stained with rabbit antibody against cleaved Caspase 3 (Cell signaling, #9661s) overnight. The stained cells were then visualized with Cy3-conjugated anti-rabbit IgG (Jackson ImmunoResearch Laboratory).

3-(4,5-Dimethylthiazol-2-yl)-2,5-diphenyltetrazolium bromide (MTT) cell viability assay has been described in details (14).

DNA contents Anisomycin-treated or control cells were stained by Propidium Iodide using "PI/RNase Staining Buffer" from BD Biosciences according to the manufacturer's manual.

Results

Induction of FoxP3 by anisomycin. We have recently shown that the expression of *FoxP3* cDNA leads to rapid cell death of breast cancer cell lines (7, 15). These results raised the possibility that the induction of *FoxP3* may represent a novel therapeutic approach for the treatment of breast cancer. When we screened for drugs that induce FoxP3 expression in mammary tumor cell lines, we observed a rapid induction of *FoxP3* mRNA by anisomycin. As shown in Fig. 1*A*, significant levels of the FoxP3 transcripts were induced in a mouse mammary tumor cell line, TSA, as early as 4 hours after anisomycin treatment. Similar effects were observed in another mouse mammary tumor cell line 4T1 and human breast cancer cell line MCF-7 (Fig. 1*B*), which we showed to harbor the WT *FOXP3* gene (7). In contrast, treatment of phorbol 12-myristate 13-acetate (PMA) did not result in any induction of *FoxP3* (Fig. 1*B*). Because higher doses of anisomycin can inhibit translation, we tested induction of the FoxP3 protein by Western blot. As shown in Fig. 1*C*, low doses of anisomycin induced high levels of FoxP3 protein, which indicated that activation of *FoxP3* locus can be achieved at doses that did not prevent translation of the FoxP3 protein. Importantly, the induction of FoxP3 protein can be prevented by FoxP3 shRNA. These data not only proved the specificity of Western blot but also confirmed that the accumulation of FoxP3 protein depends on induction of *FoxP3* mRNA.

Involvement of ATF2, c-Jun-NH_2-kinase in FoxP3 induction. As a first step to identify the mechanism by which anisomycin induced *FoxP3*, we treated mammary tumor cell line with anisomycin in conjunction with inhibitors of overlapping specificity, including ATF-2/c-Jun-NH_2-kinase (JNK) inhibitor SP10096 (SP), p38α inhibitor SB203580 (SB), and p41/42 MAP kinase inhibitor PD9786 (PD). As shown in Fig. 2*A*, SP completely prevented the induction of FoxP3. On the other hand, SB and PD had little effect. These data raised the possibility that ATF-2 and JNK pathways may be involved in the induction of FoxP3 by anisomycin.

To test this hypothesis, we generated lentiviral vectors expressing shRNA for *JNK1/2* or *ATF2*. The efficacy of shRNA

silencing and the effect of the silencing on anisomycin-mediated induction of *FoxP3* is shown in Fig. 2*B*. These data showed that silencing either *JNK* or *ATF2* resulted in abrogation of the induction of the *FoxP3* transcripts and protein by anisomycin. These data provide important genetic evidence for the involvement of JNK and ATF2 in anisomycin-induced *FoxP3* expression.

Interestingly, a recent study showed that mice with heterozygous deletion of the *ATF2* gene developed spontaneous mammary tumors (10). Because FoxP3 heterozygous mutants have the same phenotype, it is intriguing that ATF2 may be responsible for constitutive and/or inducible expressions of *FoxP3* in mammary epithelial cells. To address this issue, we obtained $ATF2^{+/-}$ mice from the frozen embryo bank of The Jackson Laboratory. The $ATF2^{+/+}$ and the $ATF2^{-/-}$ mice were obtained by F1 cross. A previous report indicated that the only a small fraction of the $ATF2^{-/-}$ mice survive to adulthood (11). We obtained two $ATF2^{-/-}$ females, from which we obtained two independent primary mammary epithelial cell cultures (Fig. 2*D*). The epithelial origin of the cultures was shown by the expression of CK19. Because T cells are the major source of *FoxP3* transcripts *in vivo*, we also confirmed that the primary culture has no T-cell

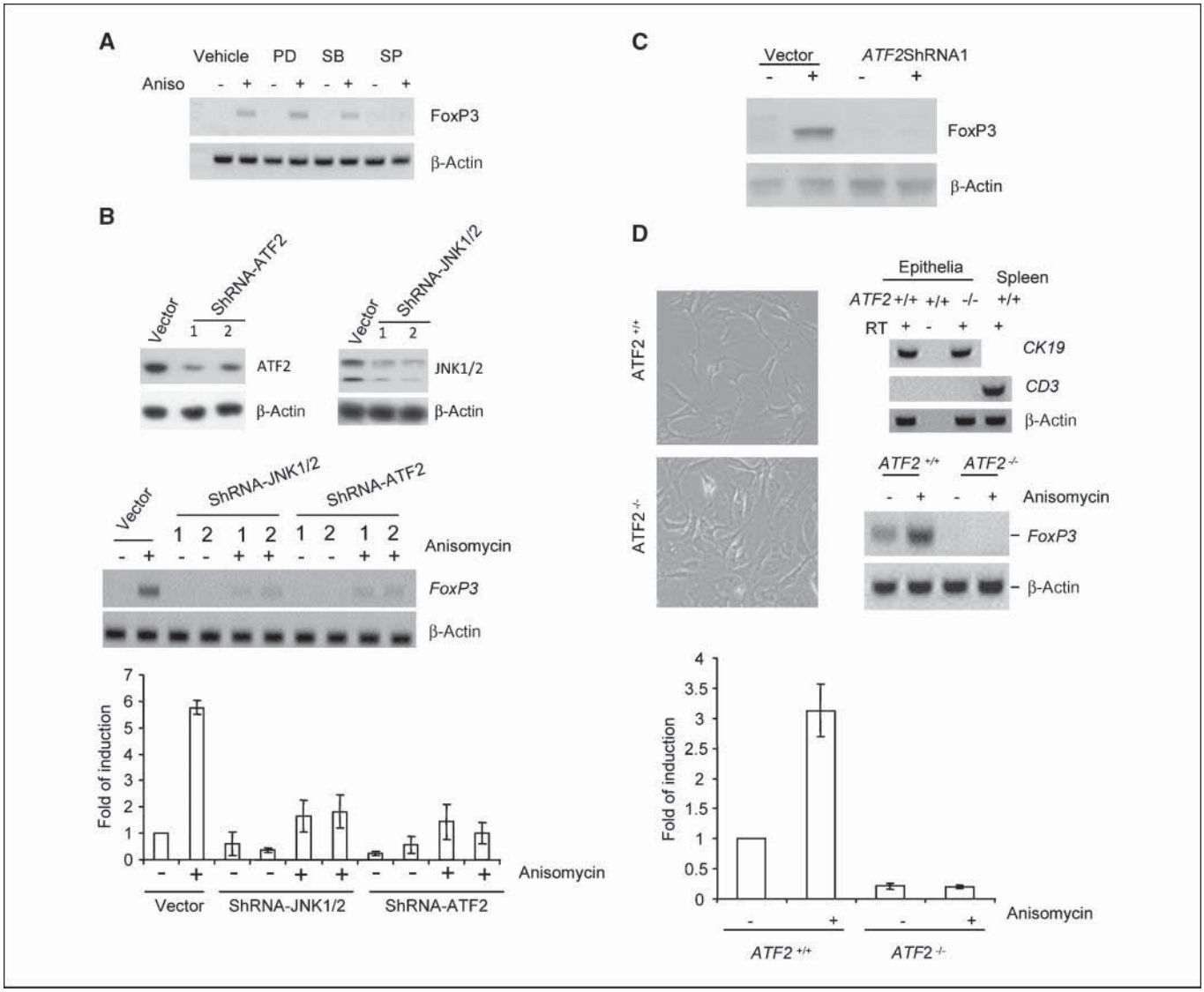

Figure 2 A critical role of ATF2 and JNK1/2 in *FoxP3* induction by anisomycin. *A,* inhibitor of JNK and ATF-2 prevented induction of *FoxP3*. 4T1 cells were stimulated with anisomycin (0.1 μg/mL) in presence or absence of inhibitors (2 μg/mL) for ATF-2 and JNK SP, SB, and PD. The induction of *FoxP3* was measured by RT-PCR 16 h after induction. *B,* effect of shRNA silencing of *ATF2* and *JNK1/2* on anisomycin-induced *FoxP3* expression. *Top,* efficacy of shRNA using lentiviral vector control or that with given shRNA, as measured by Western blot. Levels of β-actin are used as loading controls. *Middle,* RT-PCR results as determined by electrophoresis. Two independent shRNA (called 1 and 2) were used. 4T1 cells treated with either vehicle control (−) or 0.1 μg/mL of anisomycin for 16 h. *Bottom,* real-time PCR results. The *FoxP3* mRNA levels were determined by RT-PCR as detailed in Fig. 1 legends. *C,* shRNA for *ATF2* prevented induction of FoxP3 protein, as measured by Western blot. *D,* targeted mutation of *ATF2* abrogated both constitutive and inducible expression of the FoxP3 gene in mouse mammary epithelial culture. *Top* and *middle left,* morphology of epithelial culture. Note higher cellular density of the $ATF2^{-/-}$ epithelial culture. *Top right,* the primary cell culture expressed epithelial cell marker (CK19) and had no T-cell contamination as judged by the lack of CD3 transcript. *RT,* reverse transcriptase. *Middle right,* constitutive and inducible expression of FoxP3 in $ATF2^{+/+}$ but not $ATF2^{-/-}$ cultures. *Bottom,* real-time PCR quantitation of FoxP3 induction. *Columns,* means of three independent experiments; *bars,* SD. All data have been repeated at least thrice.

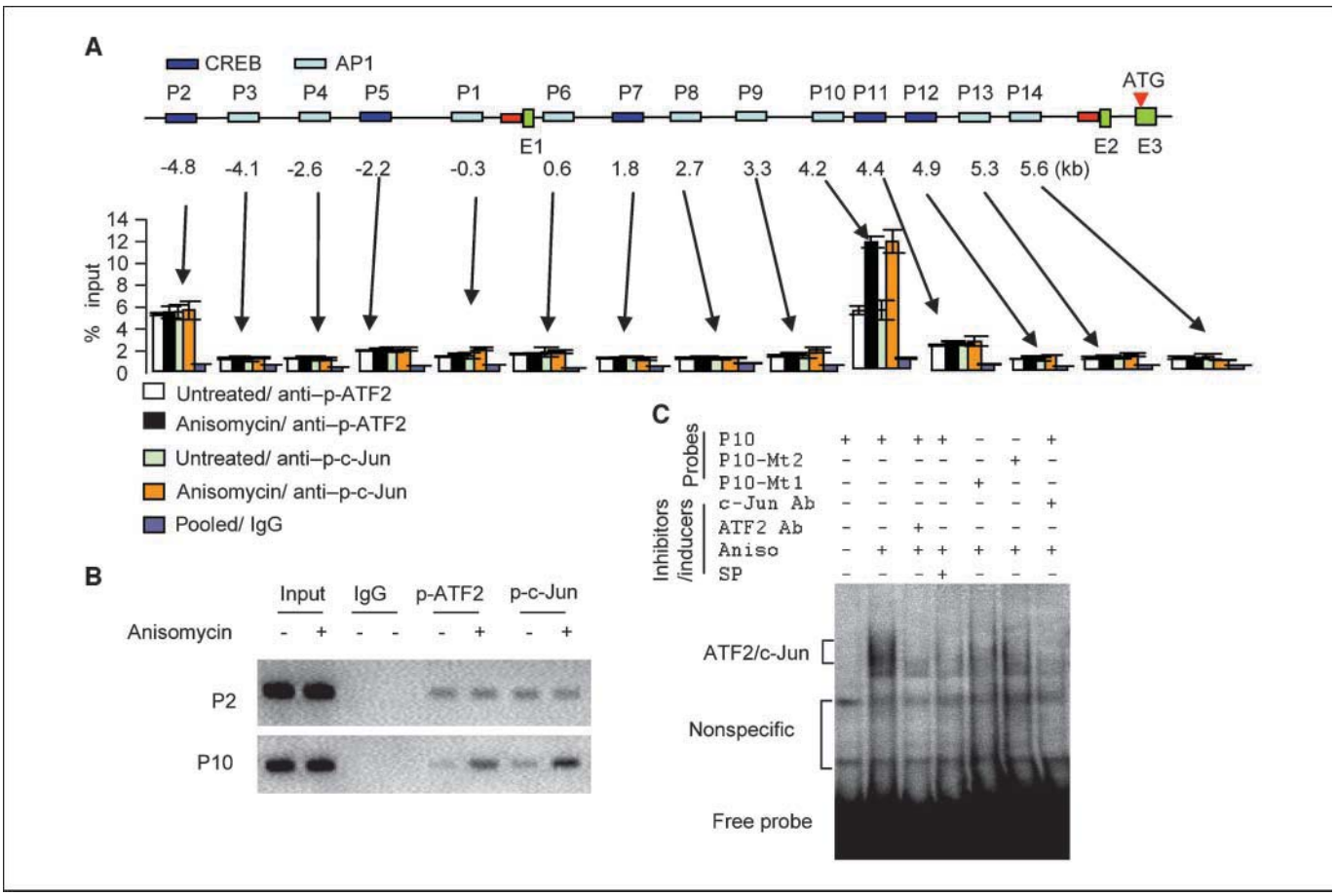

Figure 3. Identification of *cis*-elements that interact with ATF2/c-Jun heterodimer. *A* to *C,* ChIP scanning of potential c-Jun and ATF2 binding sites. The 4T1 cells were treated with either vehicle control or anisomycin for 2 h. The chromatin was cross-linked with paraformadehyde and precipitated with either control IgG, anti–phospho-ATF2, or anti–phospho-c-Jun. The amounts of DNA were quantified by PCR. *A,* quantitative analysis of the ATF2 and c-Jun binding sites in the FoxP3 locus. *Top,* the genomic structure of the 5′ of the *FoxP3* locus. The DNA quantitation was shown in the bar graph (*bottom*). Data shown are means of triplicate samples and have been repeated thrice. *B,* PCR amplification of *FoxP3* sequences P2 and P10 in ChIPs from anisomycin-treated and untreated cells. Note that although the binding of P10 to ATF2 and c-Jun are inducible, that of P2 was largely unaffected by anisomycin. *C,* the ATF2 and cJun bound to the AP1 site in P10. The sequence of WT probe (*P10*) is agatggacg**tcacctac**cacatcacgg (bold letters for core AP1 sequence), that for P10-Mt1 is agatggacgtc**tgcgc**ccacatcacgg (bold letters indicate mutations), whereas that for P10-Mt2 is agatggacgtc**ga**c**gc**ccacatcacgg. The data have been repeated thrice.

contamination by the lack of CD3 transcripts (Fig. 2*D*). WT epithelial cultures expressed significant amounts of *Foxp3* transcripts, which were further induced by the treatment of anisomycin. *ATF2*$^{-/-}$ cells had no detectable *FoxP3* transcripts and did not express *FoxP3* after stimulation by anisomycin. These data revealed an essential role for ATF2 in both constitutive and inducible expressions of *FoxP3* in normal epithelial cells. On the other hand, the thymocytes from the ATF2$^{-/-}$ mice had normal number of CD4^{+}FoxP3^{+} T cells (data not shown). Therefore, the function of ATF2 in *FoxP3* expression seems to be epithelia specific.

Identification of the *FoxP3* enhancer associated with ATF2 and c-Jun. To study the mechanism of ATF2/JNK-mediated induction of FoxP3, we carried out ChIP to identify an anisomycin-inducible binding site of the *FoxP3* locus. To identify specific ATF2 binding sites, we treated the 4T1 cell line with or without anisomycin and carried out ChIP with either control IgG or anti–p-ATF2 antibodies. Because JNK regulate transcription by phosphorylation of c-Jun (16), we used anti–phospho-c-Jun antibodies in the ChIP. To identify the *FoxP3* sequence associated with p-ATF2 and p-c-Jun, we first analyzed the 5′ sequence of the *FoxP3* gene and identified 14 potential AP1 and cAMP-responsive element binding protein sites. PCR primers were designed across the 10.4 kb regions, and the amounts of each PCR product were normalized against that amplified from the input DNA. The quantitative real-time PCR results were shown in Fig. 3*A*, whereas the PCR products from two major peaks were shown in Fig. 3*B*. These data reveal two potential sites for ATF2/cJun interaction. The first is hereby called P2, which is 4.8 kb 5′ of exon 1. The second and the stronger binding site P10 is 4.2 kb 3′ of exon 1. Importantly, whereas the P2 ATF2/cJun association is not inducible by anisomycin, the P10 binding is enhanced by >2-fold by anisomycin. Moreover, comparison of mouse and human FoxP3 sequence revealed that the P10, but not the P2 site, is highly conserved (Supplementary Fig. S1). Therefore, we focused on the potential significance of P10 as the site for p-ATF2 and p-cJun interaction.

Sequencing comparison identified a typical AP1 site within the P10 (Supplementary Fig. S1). To directly show interactions of ATF2 and c-Jun to the *FoxP3* promoter, we radiolabeled an

oligonucleotide probe containing conserved AP1 site as well as two control oligos with mutations in the AP1 site and tested their binding to nuclear extracts. As shown in Fig. 3*C*, the nuclear extracts from anisomycin-treated, but not those from the untreated, 4T1 cells showed strong interaction with the WT P10 probe. The specificity was confirmed as mutations in the AP1 site significantly reduced the binding. Furthermore, the involvement of ATF2 and c-Jun was shown as their specific antibodies abolished the binding of nuclear extracts to WT probe. Thus, both ChIP and electrophoresis mobility-shift assay identify a specific activator protein (AP1) site with 4.2 kb 3′ of the TSS, which binds to both p-ATF2 and p-cJun by anisomycin-inducible fashion.

To test whether the P10 sequence was a functional *FoxP3* enhancer, we generated a series of constructs consisting of the basal promoter and putative enhancer elements. As shown in Supplementary Fig. S2, a 265 bp sequence 5′s of TSS of the *FoxP3* locus plus 50 bp down-stream of TSS is sufficient to convey a significant basal promoter activity. This fragment is therefore chosen to measure the enhancer activity. As shown in Fig. 4, addition of three copies of P2 fragment increased the promoter activity by ~2-fold, which suggests that P2 is at best a weak enhancer. Inclusion of three copies of P10 sequences, however, increased the Foxp3 promoter activity by 10-fold. Surprisingly, this seems unidirectional as the inversion of the P10 fragment eliminated its enhancer activity. Moreover, the involvement of AP1 site in P10 was confirmed as a mutation of the AP1 site significantly reduced the enhance activity. Moreover, addition of P2 to P10 failed to further enhance the promoter activity. Taken together, our data showed that anisomycin induced ATF2/c-Jun interaction with a specific enhancer within the intron 1 of the FoxP3 gene.

A critical role for *ATF2-FoxP3* pathway in anisomycin-induced apoptosis and the therapy of breast cancer. Our recent studies have shown that the induced expression of FoxP3 caused apoptosis of breast cancer cell lines (7, 11, 15). To determine whether anisomycin treatment caused apoptosis of breast cancer cells, we measured the cytotoxic effect of anisomycin on several of breast cancer cell lines, by MTT assay. As shown in Fig. 5*A*, both mouse (TSA) and human breast cancer cell lines (BT474, MCF-7) were highly susceptible to anisomycin, with an IC_{50} between 50 and 100 ng/mL. The reduced viability is due to apoptosis as revealed by the increased expression of active caspase 3 in TSA cells (Fig. 5*B, top*) with less than 2C DNA contents (Fig. 5*B, bottom*). Given the critical role for ATF2 in *FoxP3* induction, we tested the contribution of ATF2 to anisomycin-induced cell death by comparing the dose response to anisomycin in cells transfected with either vector alone or those with *ATF2* shRNA. As shown in Fig. 5*C* and *D, ATF2* and *FoxP3* shRNAs increased resistance to anisomycin by nearly 3-fold. These data show a critical role for the ATF2-FoxP3 pathway in anisomycin-induced cell death of breast cancer cells.

To test whether induction of FoxP3 by ATF2-FoxP3 pathway can be explored for breast cancer therapy, we injected the TSA cell line into the mammary pad. Seventeen days later, when the cancer cells established locally, the mice were treated with either vehicle control or anisomycin. As shown in Fig. 6, the growth of the TSA tumor cells in syngeneic mammary pad is abrogated by anisomycin. These data show the potential of ATF2-FoxP3 pathway in the therapeutic development for breast cancer.

Discussion

FOXP3 is an X-linked gene that is subject to X-inactivation (7, 17). Our inquiry into the high incidence of spontaneous mammary tumors in mice heterozygous for the *Scurfy* mutation led to the identification of it as the first X-linked tumor suppressor for

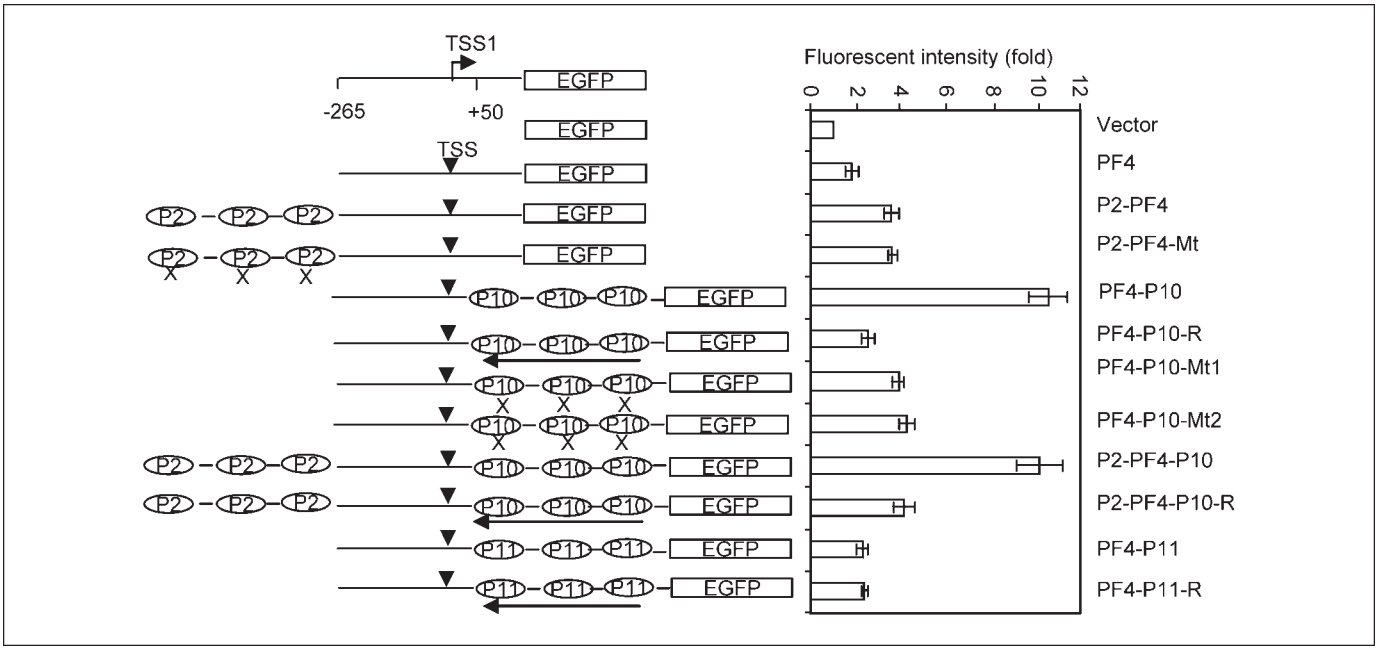

Figure 4. Enhancer activity of the ATF2/cJun binding sites in transcription of *FoxP3*. Quantitative analysis of enhancer activity. *Left,* configurations of the constructs used, including the basal promoter regions used (PF4); *right,* fluorescence intensity as measured by flow cytometry. The promoter activities were normalized by the following formula: (GFP fluorescence sample/GFP fluorescence control)/(renila luciferase activity sample/renila luciferase control). The promoter-less GFP construct is used as control. *Columns,* means of triplicates, repeated thrice; *bars,* SD.

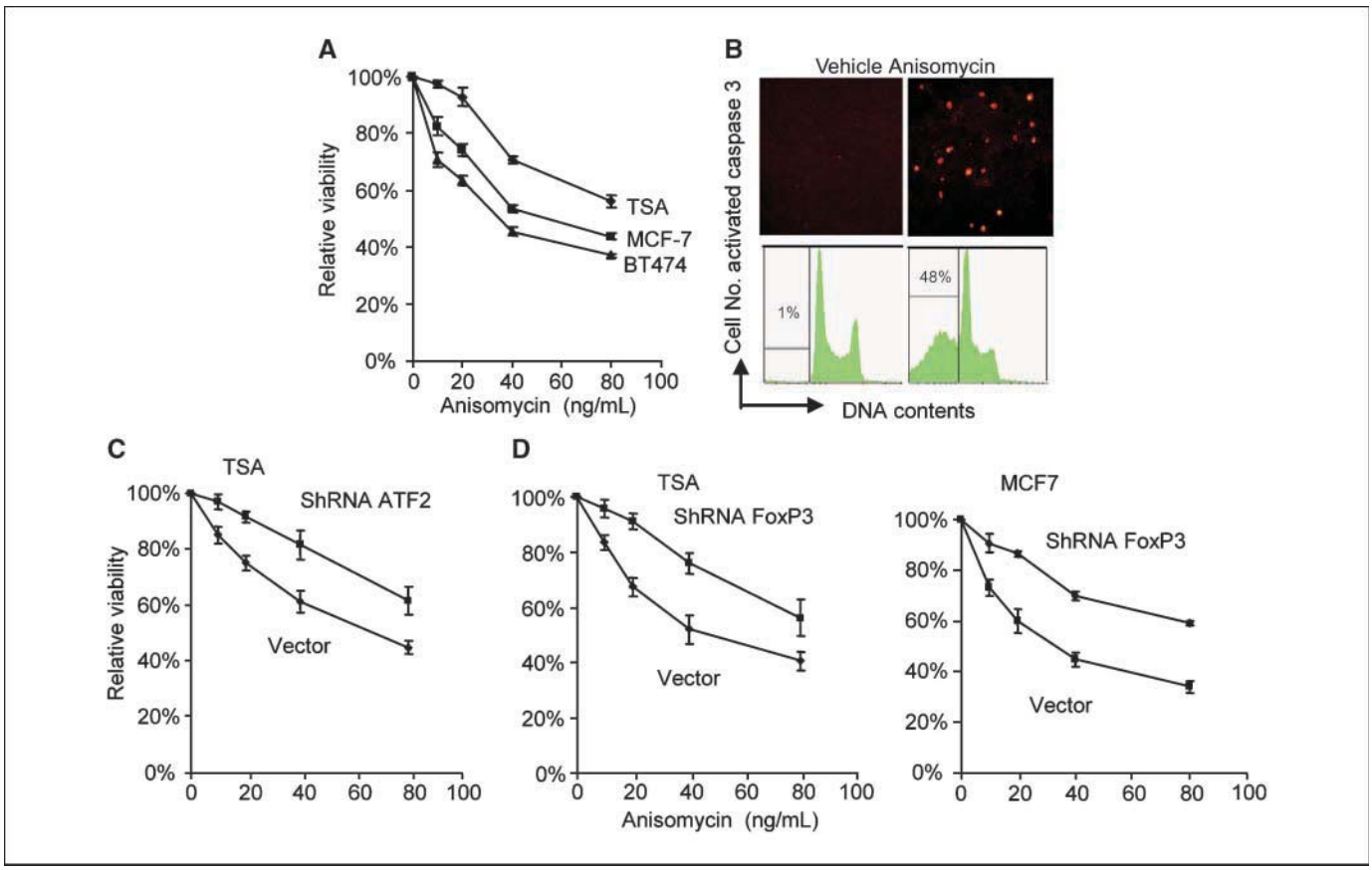

Figure 5. ATF2-FoxP3 pathway induces apoptosis of breast cancer cells. *A,* growth inhibition of mouse and human breast cancer cell lines by anisomycin, as determined by MTT assay. Mouse cell line (10^4/well; TSA) or human breast cancer cell lines TB474 or MCF7 were cultured in the presence of given concentration of anisomycin for 48 h. The amounts of viable cells were determined by MTT assay, with viability of the untreated cells defined as 100%. *Points,* means of triplicate samples, repeated thrice; *bars,* SD. *B,* anisomycin induction of apoptosis in TSA cell line at 24 h after treatment. *Top,* staining of activated caspase 3; *bottom,* DNA contents. The % of gated cells was apoptotic based on their sub-2C DNA contents. Data shown have been repeated thrice. *C,* requirements for ATF2 in growth inhibition of TSA by anisomycin. *D,* requirement for FoxP3 in growth inhibition TSA (*left*) and MCF-7 cells (*right*) by anisomycin. The indicated cell lines were transduced with lentiviral vector encoding either scrambled shRNA of shRNA specific for *ATF2* or *FoxP3*. The transfected cells were enriched by short-term treatment of blastcidin at a dose of 6.5 μg/mL and subject to treatment of different doses of anisomycin. The viability was measured by MTT assay. *Points,* means of triplicates, repeated thrice; *bars,* SD.

breast cancer in mouse and in woman (7). FOXP3 acts as a transcriptional repressor of oncogenes such as *ErbB2* and *SKP2* (7, 15). Moreover, ectopic expression of FOXP3 cause an apoptosis of breast cancer cells (7). These data showed that the induction of FOXP3 in the tumor cells may prove valuable for the treatment of breast cancer.

Because the one WT allele was not irreversibly inactivated in the overwhelming majority of breast cancer samples analyzed (7), it is theoretically possible to reactivate the expression of *FOXP3* locus for the treatment of breast cancer. The data presented herein showed such reactivation by anisomycin.

We observed that anisomycin, a drug commonly used to activate MAP kinases, rapidly induced FOXP3 expression in multiple breast cancer cell lines tested. Using shRNA specific for *Jnk* and *Atf2*, we showed that the *Jnk* and *Atf2* genes are required for the induction of *FoxP3* expression. Moreover, biochemical analysis allowed us to identify critical *cis*-element involved in the induction of *FoxP3* and that this *cis*-element interacts with c-Jun and *ATF2* to cause the activation of the *FoxP3* gene. It is worth considering whether the effect of anisomycin can be related to reactivation of X-inactivated *FoxP3*, given recent reports of chromatin modification-dependence of c-Jun–induced transcriptions (18, 19).

Using mammary epithelial culture isolated from WT and *ATF2*$^{-/-}$ mice, we showed that the targeted mutation of *Atf2* not only reduced the basal levels of *FoxP3* transcripts in the mammary epithelial cells, but also eliminated its induction by anisomycin. Therefore, ATF2 plays an essential role in both constitutive and inducible expression of *FoxP3*. It is of great interest to note that mice heterozygous for *Atf2*-null allele spontaneously developed mammary tumors (10). The similarity in tumor onset suggests that the lack of *FoxP3* expression may be an underlying cause for the spontaneous mammary tumors, although the *Atf2*$^{+/-}$ mice available to us is in 129/SV background, which is not suitable to address this issue.

FOXP3 is expressed in both T cells and epithelial cells (7, 20, 21). Because the majority of the *Atf2*$^{-/-}$ mice die shortly after birth (11), a systemic analysis of the effect on expression of FOXP3 in the T-cell lineage remained to be determined. However, our preliminary analysis suggested that *Atf2* is not essential for *FOXP3* expression in the thymocytes (data not shown). Therefore, ATF2 may play different roles in different lineages. Consistent with this notion, both *cis*-element and the *trans*-activating factors identified here differ from what were reported in *FoxP3* induction in T cells (22–25).

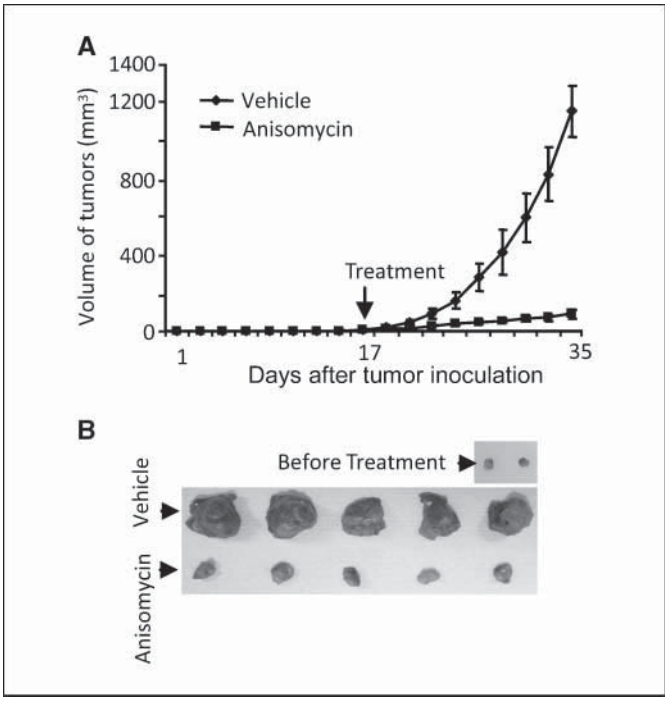

Figure 6. Anisomycin conferred significant therapeutic effect for established mammary tumor in mice. TSA cells (5×10^5) were injected into mammary fat pads of syngeneic BALb/c mice. After 17 d of injection, the mice with palpable tumors were randomly grouped and treated with anisomycin or vehicle control i.p., every 2 d for 8 times, at a dose of 0.5 mg per mouse. The dose used did not give obvious side effects and was ~1/20 of LD50 in the mice. The tumor diameters were derived from the average of largest diameters in two dimensions. The tumor volumes defined as $0.75\pi r^3$, where r is radius. *A,* the growth kinetics is shown; *B,* photographs of tumors before, and at the end of treatments were shown at the bottom. Similar therapeutic effects have been observed in three independent experiments.

Finally, an important but unresolved issue is how to reactivate tumor suppressor function in the tumor cells. Classic tumor suppressors are inactivated by two irreversible hits (2). Therefore, despite an elegant recent approach (9), restoring the function of classic tumor suppressors remains a major challenge for cancer therapy. On the other hand, recent data from our group and that of another indicated that X-linked tumor suppressor genes are subject to X-inactivation (7, 8). Because X-inactivated genes are not subject to selection during tumor growth and because deletion and mutation found in the majority of the cases are heterozygous (7, 8), it may be possible to reactivate *FOXP3* for the treatment of breast cancer. In this regard, we have shown that anisomycin cause apoptosis in an ATF2- and FOXP3-dependent manner. Moreover, the doses used here do not interfere with protein translation and cause no obvious side effect, yet the drug causes dramatic inhibition of growth of established mammary tumors in syngeneic hosts. Although more work is needed to evaluate the potential for anisomycin for breast cancer treatment, our data suggest that one may be able to reactivate X-linked tumor suppressor genes for cancer treatment.

Disclosure of Potential Conflicts of Interest

No potential conflicts of interest were disclosed.

Acknowledgments

Received 3/4/09; revised 4/22/09; accepted 5/6/09; published OnlineFirst 7/7/09.

Grant support: National Cancer Institute, Department of Defense, and American Cancer Society.

The costs of publication of this article were defrayed in part by the payment of page charges. This article must therefore be hereby marked *advertisement* in accordance with 18 U.S.C. Section 1734 solely to indicate this fact.

We thank Lynde Shaw and Todd Brown for assistance.

References

1. Hanahan D, Weinberg RA. The hallmarks of cancer. Cell 2000;100:57–70.
2. Knudson AG, Jr. Mutation and cancer: statistical study of retinoblastoma. Proc Natl Acad Sci U S A 1971;68:820–3.
3. Fearon ER, Vogelstein B. A genetic model for colorectal tumorigenesis. Cell 1990;61:759–67.
4. Hollstein M, Sidransky D, Vogelstein B, Harris CC. p53 mutations in human cancers. Science 1991;253:49–53.
5. Herman JG, Baylin SB. Gene silencing in cancer in association with promoter hypermethylation. N Engl J Med 2003;349:2042–54.
6. Spatz A, Borg C, Feunteun J. X-chromosome genetics and human cancer. Nature reviews 2004;4:617–29.
7. Zuo T, Wang L, Morrison C, et al. FOXP3 is an X-linked breast cancer suppressor gene and an important repressor of HER-2/ErbB2 oncogene. Cell 2007;129:1275–86.
8. Rivera MN, Kim WJ, Wells J, et al. An X chromosome gene, WTX, is commonly inactivated in Wilms tumor. Science 2007;315:642–5.
9. Bykov VJ, Issaeva N, Shilov A, et al. Restoration of the tumor suppressor function to mutant p53 by a low-molecular-weight compound. Nat Med 2002;8:282–8.
10. Maekawa T, Shinagawa T, Sano Y, et al. Reduced levels of ATF-2 predispose mice to mammary tumors. Mol Cell Biol 2007;27:1730–44.
11. Reimold AM, Grusby MJ, Kosaras B, et al. Chondrodysplasia and neurological abnormalities in ATF-2-deficient mice. Nature 1996;379:262–5.
12. Wang CY, Cusack JC, Jr., Liu R, Baldwin AS, Jr. Control of inducible chemoresistance: enhanced anti-tumor therapy through increased apoptosis by inhibition of NF-κB. Nat Med 1999;5:412–7.
13. Im H, Grass JA, Johnson KD, Boyer ME, Wu J, Bresnick EH. Measurement of protein-DNA interactions *in vivo* by chromatin immunoprecipitation. Methods Mol Biol 2004;284:129–46.
14. Wang Y, Liu Y, Wu C, McNally B, Liu Y, Zheng P. Laforin confers cancer resistance to energy deprivation-induced apoptosis. Cancer Res 2008;68:4039–44.
15. Zuo T, Liu R, Zhang H, et al. FOXP3 is a novel transcription repressor for the breast cancer oncogene SKP2. J Clin Invest 2007;117:3765–73.
16. Su B, Jacinto E, Hibi M, Kallunki T, Karin M, Ben-Neriah Y. JNK is involved in signal integration during costimulation of T lymphocytes. Cell 1994;77:727–36.
17. Tommasini A, Ferrari S, Moratto D, et al. X-chromosome inactivation analysis in a female carrier of FOXP3 mutation. Clin Exp Immunol 2002;130:127–30.
18. Rahman I. Oxidative stress and gene transcription in asthma and chronic obstructive pulmonary disease: antioxidant therapeutic targets. Curr Drug Targets 2002;1:291–315.
19. Tsai CL, Li HP, Lu YJ, et al. Activation of DNA methyltransferase 1 by EBV LMP1 Involves c-Jun NH(2)-terminal kinase signaling. Cancer Res 2006;66:11668–76.
20. Chen GY, Chen C, Wang L, Chang X, Zheng P, Liu Y. Cutting edge: Broad expression of the FoxP3 locus in epithelial cells: a caution against early Interpretation of fatal inflammatory diseases following *in vivo* depletion of FoxP3-expressing cells. J Immunol 2008;180:5163–6.
21. Fontenot JD, Gavin MA, Rudensky AY. Foxp3 programs the development and function of CD4+CD25+ regulatory T cells. Nat Immunol 2003;4:330–6.
22. Floess S, Freyer J, Siewert C, et al. Epigenetic control of the foxp3 locus in regulatory T cells. PLoS Biol 2007;5:e38.
23. Kim HP, Leonard WJ. CREB/ATF-dependent T cell receptor-induced FoxP3 gene expression: a role for DNA methylation. J Exp Med 2007;204:1543–51.
24. Tone Y, Furuuchi K, Kojima Y, Tykocinski ML, Greene MI, Tone M. Smad3 and NFAT cooperate to induce Foxp3 expression through its enhancer. Nat Immunol 2008;9:194–202.
25. Venuprasad K, Huang H, Harada Y, et al. The E3 ubiquitin ligase Itch regulates expression of transcription factor Foxp3 and airway inflammation by enhancing the function of transcription factor TIEG1. Nat Immunol 2008;9:245–53.